A PROBABILISTIC MODEL FRAMEWORK FOR HOLISTIC LIFE-CYCLE DESIGN OF BUILDINGS

by

Seadon Chui

B.A.Sc., The University of British Columbia, 2016

A THESIS SUBMITTED IN PARTIAL FULFILLMENT OF
THE REQUIREMENTS FOR THE DEGREE OF

MASTER OF APPLIED SCIENCE

in

THE FACULTY OF GRADUATE STUDIES
(Civil Engineering)

THE UNIVERSITY OF BRITISH COLUMBIA
(Vancouver)

October 2018

The following individuals certify that they have read, and recommend to the Faculty of Graduate and Postdoctoral Studies for acceptance, a thesis/dissertation entitled:

A Probabilistic Model Framework for Holistic Life-Cycle Design of Buildings

submitted by Seadon Chui in partial fulfillment of the requirements for the degree of Master of Applied Science

in Civil Engineering

Examining Committee:

Terje Haukaas, Civil Engineering

Supervisor

Sheryl Staub-French, Civil Engineering

Supervisory Committee Member

Supervisory Committee Member

Additional Examiner

Additional Supervisory Committee Members:

Supervisory Committee Member

Supervisory Committee Member

Abstract

The goal of the research described in this thesis is to develop a program that assists designers in designing highly efficient buildings. Rts is a model framework software that performs holistic life-cycle analysis and contains algorithms and data used to calculate relevant costs. Compatibility with building information models allows Rts to interface with other design software, while model interchangeability allows for the application of new relevant research.

Holistic life-cycle cost assessment is useful for quantifying various outcomes of a building design, such as construction cost and environmental impact. It allows for single-objective optimization by weighing these multiple outcomes objectively. Different costs have been categorized and are calculated in different models, with the existing models reviewed in this thesis. New models for construction cost, based off costing data, and concrete maintenance, using carbonation theory, have been developed.

A parametric study was performed to make preliminary observations and verify the accuracy of the models. It was found that operating costs contribute a major portion, 33%, of the total direct cost of a building, in agreement with existing literature. Furthermore, environmental impacts, particularly those resulting from emissions during operation, also contribute a large portion of total cost, at 36%. Additionally, transporting construction materials from overseas results in a dramatic increase of the environmental cost of construction, and renewable energy sources lead to a much lower total life-cycle cost. Other variables studied include the depth of concrete cover, and the influence of the discounting rate and design building life.

Lay Summary

A computer program, Rts, was extended to estimate the total cost of a building over its lifetime. Factors such as safety and environmental impact are also converted to costs and included in the total. The program itself is described in this thesis. Equations needed to calculate these costs are also reviewed, along with the development of new equations. Finally, a parametric study was performed to understand how different costs contribute to the total and to observe what happens when variables like the daily electricity demand are changed.

Preface

This thesis is original, unpublished work by the author. None of the text of the thesis is taken directly from previously published articles.

The program Rts was developed by Mojtaba Mahsuli and Dr. Terje Haukaas. Some of the models review in Chapter 3 were developed by Gurvinder Gill and implemented by Dr. Terje Haukaas. Additionally, the building information model import feature described in Chapter 2 was developed by Stevan Gavrilovic.

Table of Contents

List of Tables

List of Figures

Acknowledgements

I express my gratitude to my supervisor Dr. Terje Haukaas for his enduring patience and support in the creation of this thesis. I am thankful for the many interesting discussions we had during the course of my studies, as well as his advice and insight on a career in academia. Thanks also to Dr. Sheryl Staub-French for agreeing to be the second reader of this thesis.

I also acknowledge my colleagues in the reliability research group, Steve and Rodrigo, for their insight during our meetings on research direction. Special thanks to Steve for answering numerous emails about coding and debugging when I had trouble.

Finally, thank you to my parents for never ceasing to motivate me in my studies. Their love and support made this thesis possible. Thanks also to my sister for helping me with some of my ideas.

To my parents

Chapter 1: Introduction

Some of the most famous landmark structures, like the Great Pyramids, were designed by ancient architects with nothing more than their own experience. Throughout history, the work of renowned engineers and mathematicians has gifted modern structural engineers with tools such as calculus, Euler-Bernoulli beam theory, and the finite element method. We can now design structures that behave as we desire with great accuracy, but what exactly should we be aiming for in our designs?

Modern society faces many issues related to structures and buildings, including their impact on the natural environment, and the availability of housing in a reality with limited resources. These, along with personal preferences of occupants, push for buildings that optimize for an ever-growing list of objectives. To this end, this work describes the holistic design problem, and a software framework developed to address it.

1.1 Objectives and Methodology

Current structural design practice methodology typically attempts to minimize the volume of construction material, while meeting safety guidelines set by design codes. One of the weaknesses of this methodology is that it does not allow for the inclusion of other design factors, such as environmental impact or operating costs, for optimization by the designer. Hence, the overarching problem that this research attempts to address is how to incorporate many different concerns in structural design.

The overall goal of the current research is to implement a holistic design optimization software.

The purpose of this software, Rts, is to provide the most efficient structural design, based not only on construction costs, but operating costs, environmental impact, safety, and other direct and indirect outcomes. The objectives of the current research are to understand and describe Rts, develop and implement new models to fill existing gaps, and test the accuracy sensitivity of the program's models and parameters.

To meet the research objectives, Rts' source code was accessed using Qt Creator (The Qt Company, 2016). A study of the existing framework was made to understand how it functions, the current state of the models, how they function as part of Rts, and what models were still needed. Two new models were selected for development and implementation: a new construction cost model, and a model for the deterioration and maintenance of concrete components. To develop these new models, concrete construction processes and the deterioration of concrete components were researched. They were then added to the Rts source code in the C++ programming language using Qt Creator. Finally, simulations were run in Rts using input files containing the details for a small building, and different parameters were varied to observe their effects on the building's outcomes, such as the total cost.

1.2 Research Contribution

The first contribution of this research was the development and implementation of two new models for holistic life-cycle costing. A model for the detailed costing of concrete component construction was developed, as was a model that schedules and provides the cost of maintenance for exposed concrete components.

The other main contribution was the conclusions and comments made on the results of the parametric studies. These showed that Rts produces results comparable to those found in literature, and how environmental concerns factor in as costs compared to the direct costs of a building. Additional comments were made on subjects including energy usage, the transportation of construction materials, and concrete cover depth.

1.3 Thesis Overview

One of the intents of this research is to describe Rts. Chapter 2 describes how to use Rts and the framework in Rts for the implementation of the models used to calculate life-cycle costs. Features in Rts for modelling, such as plug-and-play functionality and BIM-compatibility, are also explained.

Chapter 3 is dedicated to explaining cost modelling in Rts. A general overview of holistic life-cycle costing is also given, to inform the reader how it is to be performed in Rts. The literature background of the existing and new models, the expressions and parameters in them, and how they fit in to holistic life-cycle analyses are all described. Also, structural design methodology is reviewed to explain why holistic life-cycle assessment is necessary in the context of modern design. The concept of converting non-cost outcomes like greenhouse gas emissions in to costs is also explained and justified.

A parametric study was performed on an example building using Rts, and the results are discussed in Chapter 4. Observations regarding the major costs contributing to the total life-cycle cost are made to see their relative significance. Various parameters are varied to see how sensitive the total cost is to them, and how they affect the total cost. Some conclusions are made in comparison to relevant studies to verify the accuracy of the models used in the study.

1.4 Background

Holistic life-cycle assessments quantify multiple outcomes such as construction cost, environmental impact, and casualties due to hazards (Gencturk, Hossain, & Lahourpour, 2016; Wen, 2001). Using these for design optimization allows for design solutions that are efficient in a holistic sense, and unconstrained by arbitrary guidelines.

Construction cost estimation is a subject commonly taught in civil engineering, following the standard practice of referring to estimating handbooks. Rts includes a construction cost model by Gill (2017) developed through linear regression of RSMeans data (Gordian, 2018), which uses component specifications such as external dimensions. However, the use of regression models requires the models to be re-calculated regularly from costing data. The use of BIM (building information model) to provide information directly to cost estimating software has been discussed (Revit, 2006). Cost-estimating software is regularly updated by third parties so that the user does not need to manually update the data. Hence, using an API to directly access the capabilities of existing BIM cost-estimating software could ensure that construction cost estimates stay up-to-date.

Environmental impact, specifically greenhouse gas emissions and energy usage, is also a heavily studied topic in modern engineering. Nordhaus (2011) studied economic prediction models to estimate the social cost of carbon, evaluating the indirect cost of atmospheric pollution. Databases such as the Inventory of Carbon and Energy (Hammond & Jones, 2008) provide estimates of the embodied energy of products. Along with data such as statistics on household energy use (Natural Resources Canada, n.d.), these are used by Rts to estimate the life-cycle environmental impact of a building.

While collapse is a factor that has always been designed for, risk has only been quantified as an outcome in recent years. Performance-based earthquake engineering (Cornell & Krawinkler, 2000) was the beginning of studying the functionality and repair costs of a building after an event. The Federal Emergency Management Agency (2015) has since extensively researched direct economic loss due to hazards. Additionally, a new type of study, resilience engineering, attempts to quantify indirect losses due to building downtime (McAllister, 2016). Gill developed a "casualty cost model" to estimate approximate costs due to injury and loss of life (Gill, 2017).

In this work, the maintenance and deterioration of concrete components is also incorporated into Rts. Concrete carbonation is a well-studied subject, as it is related to the deterioration of many older structures. Zhao (2016) wrote extensively on how concrete carbonation eventually leads to the rusting of reinforcing steel and subsequent cracking of concrete. Various models for carbonation have been proposed, typically based on Tutti's curve (Monteiro, Branco, Brito, & Neves, 2012), along with estimates of the value of the carbonation coefficient.

Mahsuli and Haukaas (2013b, 2013c) previously developed a reliability-based optimization software, Rt, which later gained structural analysis tools to become Rts. Rts was used to conduct seismic risk assessment for the Metro Vancouver region (Mojtaba Mahsuli, 2012).

Chapter 2: Rts Framework

Rts is a probabilistic analysis software for buildings developed by Dr. Terje Haukaas and associated graduate students. As introduced in Chapter 1, Rt, the core of Rts, contains and runs algorithms used for probabilistic analysis (M. Mahsuli & Haukaas, 2013a, 2013b, 2013c). Rts extends Rt to add structural analyses, optimization, network analysis, and cost estimating. It is programmed in the C++ language on the Qt Creator development platform (The Qt Company, 2016).

2.1 Rts Basics

Figure 2.1 is a screenshot showing the user interface of Rts. The main window displays analysis results, such as the sampling distribution plot in this example. On the left side is the Objects pane, with existing objects, such as a FORM model and an algebraic expression "g", in red font. Users may also use this pane to browse existing classes to create new objects. The bottom-centre window shows the Properties pane, displaying the properties of the selected object. In this example the object "theSamplingModel" has been selected, as seen in Figure 2.1 in the Objects pane. This pane shows the object's properties, also known as attributes or inputs, that the object may require, such as the maximum number of samples to be taken. The bottom-right Output pane shows output that may include numerical results, or information useful for debugging. In this example, the Output pane has tracked how long each sampling iteration took to complete, how many samples were taken, and returned the sampling results.

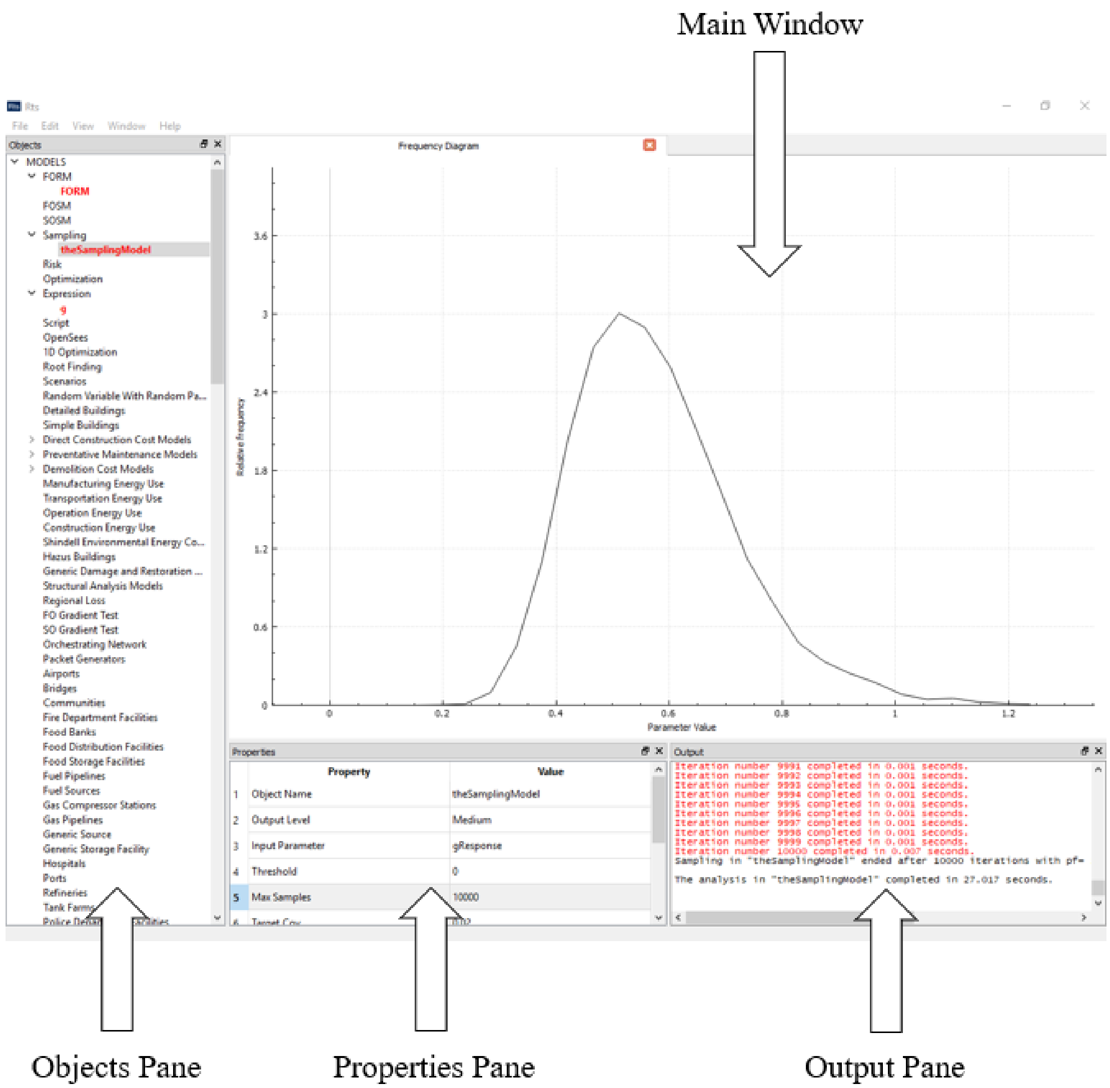

Figure 2.1 User interface of Rts, showing a completed sampling simulation model.

Rts objects consists of models and methods. Models are equations or algorithms that simulate physical phenomena, take inputs and return outputs. They are discussed further in Section 2.2. Methods, discussed in Section 2.3, are algorithms, such as line search algorithms, used by models or other methods.

Rts can take text input files to create the models, methods, and other objects used in analyses. This facilitates setting up analyses with many objects, in contrast to creating the analysis objects through the user interface. Rts creates and object from each line in the input file, which have the following syntax:

```
ClassName |ObjectName: exampleObject |Attribute1: exampleAttribute
```

For clarity, the input file examples below will include line breaks to separate different attributes. For example, the line of text that created the sampling model “theSamplingModel” in Figure 2.1 is shown here:

```
RSamplingModel
|ObjectName: theSamplingModel
|OutputLevel: Medium
|InputParameter: gResponse
|Threshold: 0
|MaxSamples: 3000000
|TargetCov: 0.02
|PlotInterval: 100
|SamplingCentre: Origin
|RandomNumberGenerator: RNG
|ProbabilityTransformation: ProbT
```

First in this input line is a declaration of the class of this object, in this example: “RSamplingModel”, the name of the sampling model class. Next, attributes such as the name, the exceedance threshold, and the maximum number of samples are given. The output level, which is an attribute of all objects, tells the program how much information about this object should be provided in the Output pane mentioned above.

Some attributes, such as “InputParameter” require inputs that are other objects. “InputParameter” is an example of models taking input from other models, which will be covered further in Section 2.2. In this example, the input parameter “gResponse” is the output produced by the model “g”. “g”, also seen in Figure 2.1, is an algebraic expression created by the text below.

```
RAlgebraicExpressionModel
|ObjectName: g
|OutputLevel: Medium
|Expression: x2/1000/x3+(x1/220/x3)^2
```

Note that “g” must be defined in the input file before “theSamplingModel” so that Rts knows what the user is giving as the input parameter. The variables in “g” are also objects, specifically, they are random variables. As before, these need to be defined before “g”, the text creating “x1” is given below.

```
RContinuousRandomVariable
|ObjectName: x1
|CurrentValue: 500
|DistributionType: Lognormal (zeta, sigma)
|Mean: 500.0000000002
|StandardDeviation: 100.0000000001
|CoefficientOfVariation: 0.2
```

The sampling model also uses a random number generator object “RNG”. “RNG” is a method, not a model, so it does not have a response object such as “RNGResponse”; its output is directly passed to the sampling model.

2.2 Rts Models

As introduced in Section 2.1, models are equations or algorithms that simulate physical phenomena. Some examples include hazard intensity and scenario models, the latter of which simulates the life-cycle of a building or network. Possible models that have not been implemented in Rts may include solar radiation or soil interaction models. Most models generate at least one output or response, which may be the quantifiable results of the phenomena they are simulating, and often require at least one input from another model. Mahsuli (2012) prescribes rules that specifically govern which algorithms or equations may be considered models in Rts.

Figure 2.2 shows a schematic demonstrating how models provide responses for other models. This example portrays an optimization model using sampling to optimize a building that is being damaged by an earthquake and a snowstorm. It is observed that, first, the occurrence model, such as a Poisson occurrence model, provides occurrence times for the magnitude model. The magnitude model provides hazard magnitudes at those times, while the location model provides the location for the earthquake. The earthquake intensity model then takes the magnitude and location provided to produce an earthquake intensity for a building. The damage model calculates the resulting damage, and produces a response or set of responses, such as repair costs and downtime. The scenario model then accumulates these into the life-cycle cost of the building. The sampling model runs the entire simulation many times with different realizations of the random variables, and finally provides these to the optimization model for analysis. Notice that all the responses that are passed represent some observable phenomena, i.e. earthquake occurrence times and earthquake intensities.

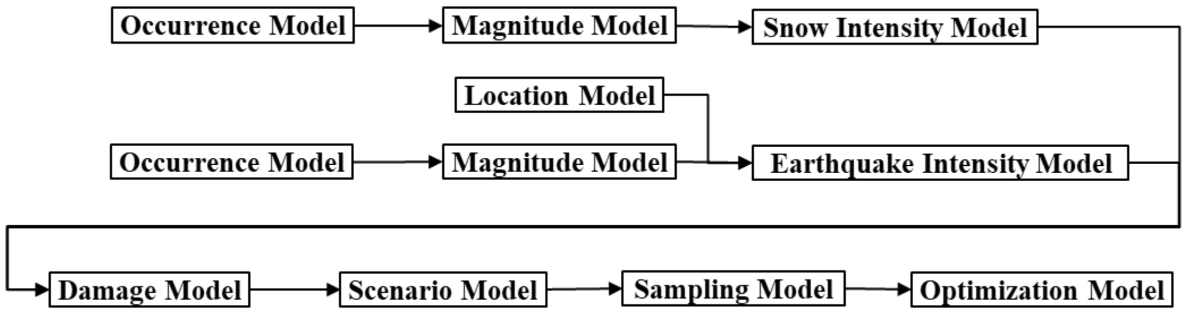

Figure 2.2 Flowchart showing a stream of model responses.

Figure 2.2 does not include the methods and other objects required for this simulation, such as the random number generator used by the sampling model, or the BIM used by the damage model. Building information models are discussed in Section 2.3.

Figure 2.3 shows how a model class, in this case RSamplingModel, requires an RResponse object, as part of the stream of model responses. In the example in Figure 2.1, this would be “gResponse”, the output of the expression “g”, as was mentioned above. In addition, it also requires several methods and non-object attributes, such as the exceedance threshold and the maximum number of samples that should be taken.

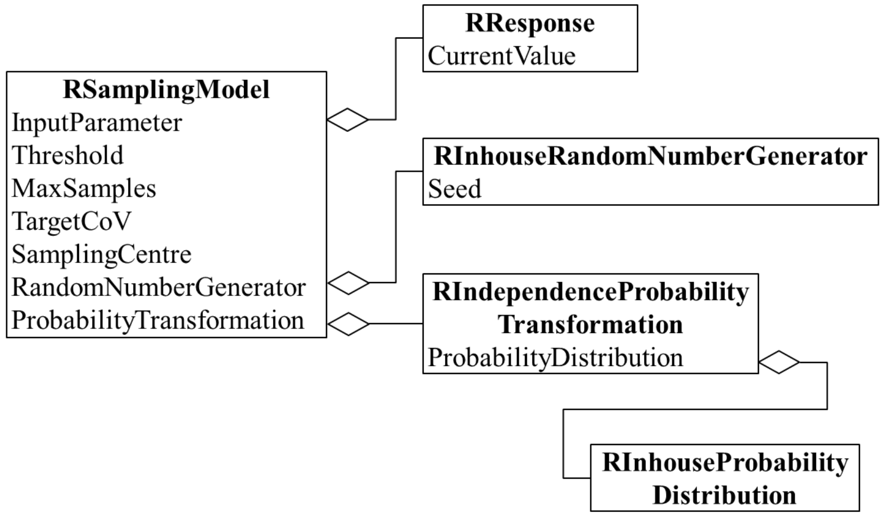

Figure 2.3 Class diagram demonstrating aggregation between methods and models.

2.3 Rts Methods

Methods are distinct from models in that they do not represent physical phenomena; rather, they perform the sub-tasks required by models or other methods. Examples of methods include linear solvers, line search algorithms, and structural analyzers.

One of the features of Rts is that, like the popular structural analysis program OpenSees (McKenna, 2011), methods of the same base class may be interchanged. Functionally this signifies that two methods that perform the same task in different manners may be used in place of each other. Figure 2.4 shows how both the Nataf and independence probability transformation classes are derived from the general probability transformation class. In the example above in Figure 2.3, the sampling model needs a probability transformation, and an independence probability transformation is given. However, a Nataf probability transformation may be used instead, or any other probability transformation the user specifies. This "plug-and-play" functionality allows users to develop their own methods and test or use them in Rts.

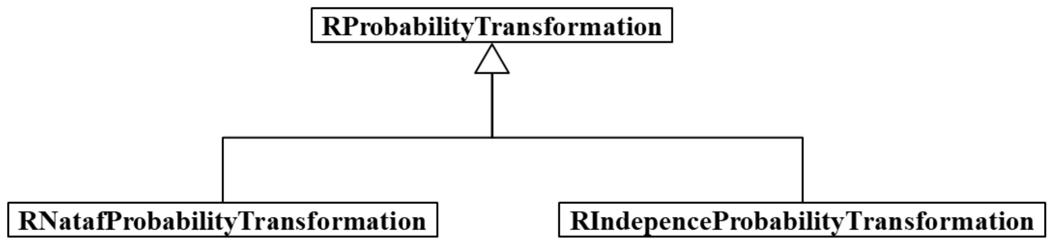

Figure 2.4 Class diagram showing inheritance of probability transformation class.

2.4 Rts Buildings

The Buildings extension of Rts encompasses the models and methods specific to structures. One of the main capabilities of this extension is to run scenarios simulating life-cycle analyses of buildings. Figure 2.5 shows a sampling analysis of a scenario model simulating a building's life-cycle cost; life-cycle analysis and the associated models are discussed further in Chapter 3. The scenario model accumulates the lifetime costs of the building and applies discounting to future costs to provide the total in present worth.

The upper portion shows a stream of models as in Figure 2.2. Additionally, other "cost models", such as the construction and demolition cost models, are also shown. These costing models are the primary focus of the current research and the later chapters of this thesis. Notice that these models all require a BIM, which provides information about the building.

Additionally, the Buildings extension adds energy-demand models, such as the manufacturing energy model. As introduced in Chapter 1, these were developed by Gill (2017) to be used in conjunction with SCAR (social cost of atmospheric release) factors (Shindell, 2015). The

SCAR coefficients are implemented in the environmental impact model, which converts the energy usages to costs.

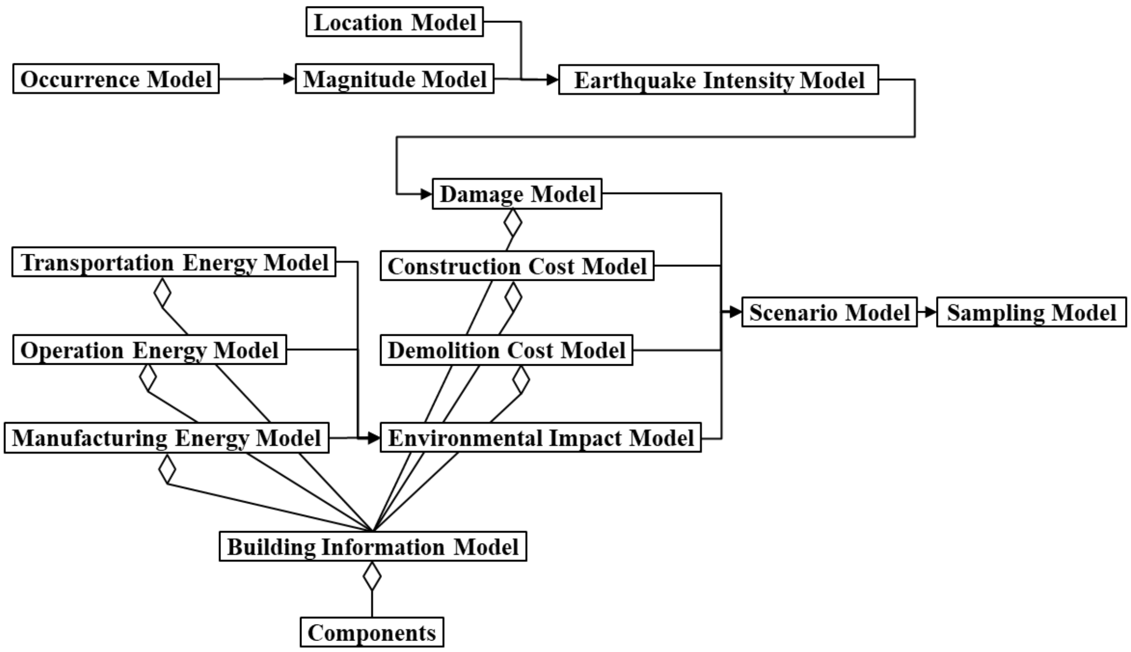

Figure 2.5 Interaction diagram showing models involved in a scenario sampling analysis.

Furthermore, the Buildings extension adds objects necessary for detailed finite element analysis. These include methods such as structural analyzers and matrix assemblers, as well as linear and nonlinear mesh elements. This feature of Rts allows for detailed damage models that can precisely model the state of a building after an event, while incorporating uncertainty in the loads.

2.5 Building Information Models

The building information model object is somewhat misleadingly named, as it is not a proper "model" in the scope of Rts. A BIM object represents a single building or structure, and primarily functions as an interface between the building models and the components, which are described in the next section. For example, most cost models call the BIM to pass either quantities related to the building, such as the total volume of concrete, or a list of the components themselves.

The BIM also has information regarding the building as a whole, such as types of occupancy or construction. Statistics-based cost models, for example the "cost of casualties" model (Gill, 2017), may rely on this broader categorization to look up values for losses or downtime.

Finally, the BIM object is also capable of reading and importing components in ifc files. Ifc files are created in BIM editors such as Revit and are the typical filetype used when working with BIMs. This functionality allows Rts to interface with programs that are expected to increase in popularity with contemporary designers.

2.6 Components

Components in Rts are all structural and non-structural components of a building. A class diagram of all currently existing components is shown in Figure 2.6. All components are divided into 1D and 2D components and are directly derived from those two subclasses.

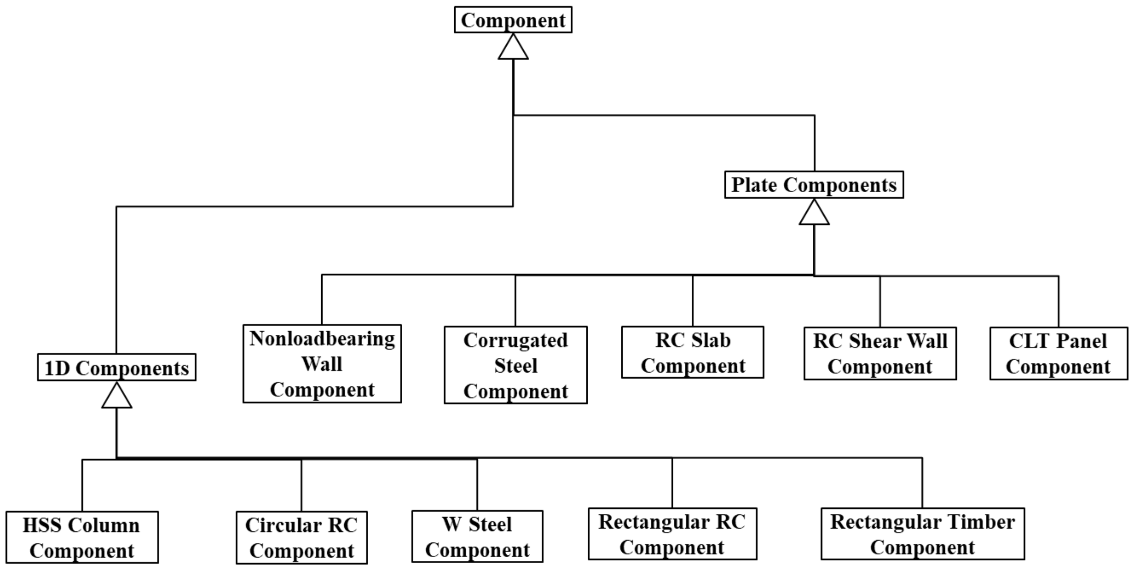

Figure 2.6 Class diagram of existing Rts components.

Rts components are considered "information-rich", as they contain the details about themselves. They do not contain the expressions or algorithms required for costing or structural analyses; these are strictly contained in the appropriate models and methods. Components contain information such as cross-sectional dimensions and steel or concrete strengths. They also return some simple quantities, such as total surface area, volumes of materials, and length, for use in cost models. For instance, concrete components return their surface area, for construction cost models to calculate the cost of the required forms.

In OpenSees, finite element objects are defined in the input file with additional associated objects representing their cross-section and their material. In Rts, the components do not themselves take any role in structural analyses. Components have a function that tells the component to create the finite element mesh object that corresponds to it, which then acts in its place for all analysis purposes. Rts components are not defined with such objects, instead, the component itself creates the cross-section and material "knowledge" objects using the information it contains. These "knowledge" objects are linked to the component's mesh object and are handled together by the structural analyzers.

The component reads information about its mesh object through its points. For example, a concrete column component has two points, one at either end. The corresponding mesh object will also have two corresponding "nodes" linked to the original points. The component can request information about its mesh through this node-point relationship, to return information such as drift for use in repair cost models.

Each component class exists with significant distinction from other existing components. For instance, rectangular and circular concrete columns only differ in the shape of their cross-section. However, this results in differences in the calculations of their construction costs, due to the use of paper-fibre circular forms compared to plywood rectangular forms. Similarly, concrete shear walls and slabs are separate due to differences in their behaviours under loading. For this reason, components that may be treated similarly in a structural analysis are contained in different classes in Rts.

Chapter 3: Cost Models

Contemporary design demands consideration of many factors, such as construction cost, environmental impact, and safety. To obtain discrete optimal solutions, the quantities of these factors must be converted to costs. This chapter aims to describe the need for holistic optimization, as well as the methodology and models that address it.

3.1 Holistic Life-Cycle Cost Assessment

Generally, the objective of modern structural design is to minimize construction costs while meeting safety guidelines specified by building codes, e.g. the National Building Code of Canada. However, due to the probabilistic nature of loads and material strengths, a building can never be considered entirely safe. Resources, both human and natural, are limited, and so safety guidelines can only practically aim to lower failure probabilities to a "safe" level.

This methodology provides owners the freedom to optimize for costs. However, the need to select target failure probabilities represents a serious shortcoming. While importance factors can be used to roughly adjust the target failure probability, major variations between buildings justify more precision. For example, a large busy theatre and a small theatre are designed with the same target failure probability. However, a collapse of the former would be a more devastating event than the latter. Whether the two buildings should have different standards of safety imposed on them is at least questionable. Especially for publicly-owned buildings, where both direct costs and the price of failure are paid by society, this shortcoming supports using a more robust methodology.

Another issue is whether immediate safety and construction cost are even the only issues of relevance. Operating costs and financial losses after an event are also important to an owner. Islam, Jollands, and Setunge (2015) found that the direct cost of operation may vary from 20% to 50% of a building's total life-cycle cost. Buildings also account for a large portion of the world's atmospheric emissions; responsible for approximately 40% of global energy use (Fowler, Rauch, Henderson, & Kora, 2010). While there is little legislation related to the environmental impact of buildings, the costs of pollution are nonetheless borne by society.

Reliability-based engineering (Enevoldsen & Sørensen, 1994; Frangopol & Maute, 2003; M. Mahsuli & Haukaas, 2013c; Royset, Der Kiureghian, & Polak, 2001) addresses the concerns regarding failure probabilities. Life-cycle reliability assessments, used in reliability-based engineering, study the risk of failure over the lifetime of a structure, thus exposing the uncertainty hidden in code-based design. Additionally, such assessments prompt a more thorough study of hazards, providing the possibility of designing against unaccounted-for events.

Studies in different fields of engineering address the second issue concerning additional stakeholder interests. The damage state and functionality of a building after an event are studied in performance-based design (Cornell & Krawinkler, 2000; Ellingwood, 2008; Mahoney & Hanson, 2012; Yang, Moehle, & Stojadinovic, 2009). Resilience engineering (McAllister, 2016; Tierney & Bruneau, 2007) further incorporates recovery time and indirect costs, important to both owners and societies. Life-cycle cost analyses (Goh & Sun, 2016) can calculate operating and demolitions costs. Environmental life-cycle analyses can estimate the atmospheric emissions of a building with reasonable accuracy (Sharma, Saxena, Sethi, Shree, & Varun, 2011). Holistic life-cycle assessments (Gencturk et al., 2016; Wen, 2001) attempt to combine these.

The result is a probabilistic multi-objective optimization problem. Marler and Arora (2004) discuss different approaches to such problems, such as Pareto sets, weighted methods, and constrained methods. Zou, Chan, Li and Wang (2007) demonstrate optimization incorporating both reliability and life-cycle costs using Pareto optimal sets. While Pareto sets allow for significant user flexibility, they require the user to weigh the benefits and costs of different objectives against each other. Multi-criteria decision matrices (Hopfe, Augenbroe, & Hensen, 2013) and analytical hierarchy processes (Das, Chew, & Poh, 2010) use weights to scale the different variables between acceptable solutions, before summing them. These approaches suffer from the possibility of excluded optimums, as well as the presence of outliers skewing the importance of those variables.

This research aims to produce unique optimal solutions to unconstrained design problems, as opposed to solution sets, indicating that a weighted sum method should be used. However, weighting methods can be subjective and biased, as the assignment of weights is determined by the user. To reduce subjectivity in selection of weights, the concept of social costing has been used. The social cost of a product is the total cost society pays (Federal Reserve Bank of San Francisco, 2002). It is the sum of the cost paid by the person making a purchase and the costs paid by the rest of society (Baumol, 1972). A relevant example might be the construction of a new building. The construction cost of the building is paid for by the owner, but the harmful effects of the resulting pollution, such as lower air quality, are borne by the public. Social costing, such as the social cost of carbon (Nordhaus, 2011) in this example, allows for the quantification of such effects as costs. This transforms the multi-objective optimization problem into a single-cost optimization problem.

The conversion of objective function outputs, such as the number of injuries due to collapse or tonnes of life-cycle atmospheric emissions, to costs allows the total cost of a structure to be estimated. In turn, this enables the design of structures considering the total social cost, that they may be optimal in a holistic sense. Costs, such as environmental damage or the risk of human injury, are positive in Rts, while benefits, such as societal function, are negative.

3.2 Scenario Model and Discounting

Holistic life-cycle cost assessment involves calculating costs associated with a building over its life-cycle and summing them. The Rts model that oversees this process is the scenario model, with the class name RScenarioModel, introduced in Chapter 2. The scenario model's inputs include a list of cost models; this list defines what costs will be included in any given life-cycle cost analysis.

Figure 3.1 shows a single scenario analysis run in Rts, with the blue line indicating the total cost of a building over its life-cycle. Notice that the total cost does not increase continuously, but in discrete increments. The scenario model evaluates all the cost models at pre-determined time instances, known as in Rts as "trigger times". Some models, such as earthquake occurrence models, return specific times at which the scenario model must perform evaluations. The scenario model also creates additional trigger times if the period between two consecutive trigger times is too long, to create a near-continuous evaluation. The maximum allowable time gap is one of the model's attributes. In the analysis shown in the figure, the scenario model has no intermediate trigger times between the start and the end and a maximum time gap of one year. This signifies that all consecutive evaluations are one year apart in time.

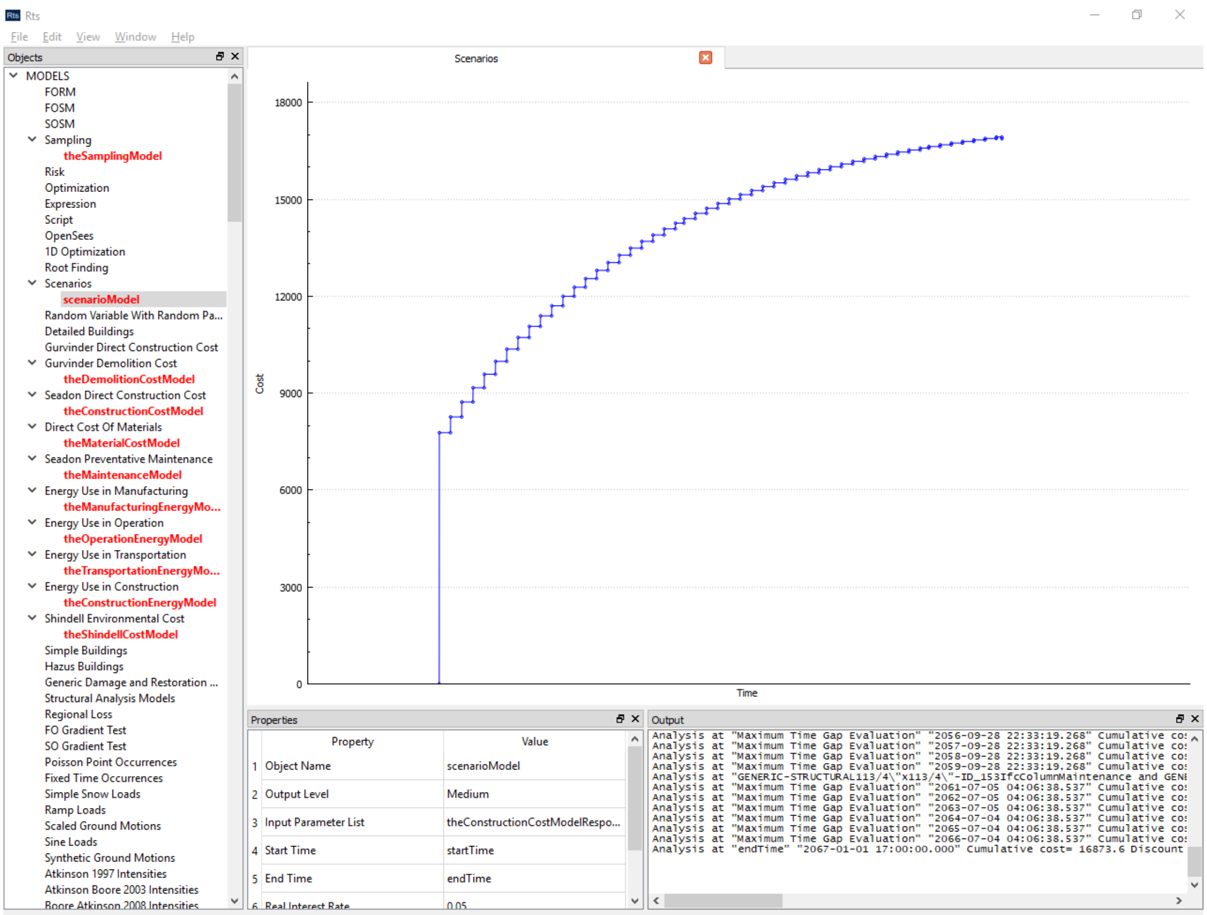

Figure 3.1 Screenshot of a scenario analysis run in Rts.

In addition to evaluating all the cost models, the scenario model also applies discounting to the costs at that time instance before adding them to the total life-cycle cost. Discounting is the conversion of future costs into present values. The scenario model in Rts uses the exponential discounting model, which is given by:

$$W_P = W_F e^{-rt} \tag{3-1}$$

where W_P and W_F are the present and future worths respectively, r is the real interest rate, and t is time. Hence, any costs that are incurred in the future, such as paying for building demolition or maintenance, are converted to present values before summation as part of the total. Notice that this expression assumes continuous discounting, as opposed to annual or monthly interest accumulation expressions with the term $(1+r)^t$. While the expressions return similar results, continuous discounting does not require input on how frequently the interest should be updated.

Discounting may be understood in two ways, as explained by Nordhaus (2007). The first, sometimes referred to as due to capital growth or the "time value of money", is because of investment. A purchase of 1 million dollars to be made in 20 years will cost less than 380 000 if that is invested today at a 5% interest rate. This is fundamentally due to investment and growth in the economy.

Discounting may also be understood to be the devaluation of future purchases because of perceived utility. People desire goods and services immediately and are willing to pay more for purchases made sooner rather than later. This preference does not result in a constant rate of interest over time. Kenley and Armstead (2004) argue that because consumer preference is not constant over time, it is more appropriate to use a non-constant-rate discounting model, such as hyperbolic discounting.

Noor (2009) argues that exponential discounting, with its constant interest rate over time, can accommodate for fluctuations in consumer behaviour through calibration. More significantly, one of the philosophies behind Rts is to remove bias to obtain optimal solutions. As such, models that mimic human behaviour are not as appropriate as utility-neutral models, such as the exponential discounting model.

There is additional debate regarding the application of discounting social costs, particularly the impacts of emissions. These costs, while having value, are not actually money, making it harder to apply the rules of discounting. Stern (2007) and Nordhaus (1994) both model the impacts of carbon emissions of future welfare to help guide government policy on reducing emissions. Stern's recommendation is that immediate and drastic action should be taken against climate change, while Nordhaus suggests that controls should be implemented gradually. Nordhaus (2007) explains that this is largely due to differences in discounting. Stern assumes near-zero discounting, with the reasoning that the cost imposed on future generations because of pollution can not be justified as being less than cost imposed on the current one. Nordhaus (2007) mentions that he uses a rate of 6%, corresponding to the empirical rate of return on capital, or capital growth rate. Nordhaus argues that, while near-zero discounting may represent an ideal scenario, some unrealistic assumptions must be made to defend it. For example, he points out that Stern does not account for competition in the global economy. He concludes that how discounting should be applied to environmental damage is still a question of great uncertainty that should not be treated as settled. In Rts, exponential discounting is applied to all costs, similar to the approach used by Nordhaus (1994), with the flexibility that other discounting models may be developed for individual costs.

3.3 Cost Modelling in Rts

Generally, cost models may be categorized in two dimensions, cost type and life-cycle phase, as listed below in Table 3.1. Direct costs are costs that the owner pays for, such as construction costs or utility bills. They also include profit-related costs, such as the revenue lost during repairs after building damage. The social costs of actions that impact the environment, or environmental costs, cover all costs related to pollution that are not explicitly paid for by the owner. The social cost of injuries and fatalities represents the cost that society pays in the case of building collapse. User-experience costs include items like the influence of aesthetics on the desirability of a residential unit and the impact on its value.

Table 3.1 Categories of cost models.

Cost Types	Life-Cycle Phases
• Direct costs	• Manufacturing phase
• External environmental costs	• Construction phase
• Costs of injuries and fatalities	• Operations phase
• User costs	• Demolition phase
	• Hazardous events

The different phases of a building's life-cycle are reasonably self-explanatory. The manufacturing phase specifically indicates the "cradle-to-gate" portion of a product's life, from the raw material source to the completed product at the manufacturing plant. Hazardous events are not an actual phase but represent the cost of the consequences and actions that might occur in response to damage or discomfort during such an event, such as repairs or injuries.

Cost models are not strictly categorized in Rts; that is, different cost models quantifying the same cost category do not necessarily have a common parent class for that category. Some cost model schemes might combine the manufacturing and construction costs into one model, others separate them. An implication of this is that the scenario model may be given any list of cost models. This allows the user to study specific models in isolation and allows for flexible model development. However, this also requires the user to have a firm understanding of life-cycle assessment and the necessary Rts models. For example, an input file line creating a scenario model might be:

```
RScenarioModel
|ObjectName: scenarioModel
|InputParameterList: theConstructionCostModelResponse;
theShindellCostModelResponse; theOperationEnergyModelResponse
|StartTime: startTime
|EndTime: endTime
|MaxTimeGap: 365
|RealInterestRate: 0.05
|OutputLevel: Medium
```

The three models in InputParameterList cover manufacturing and construction, environmental, and operating costs. Notice that it is not explained that the construction cost model also includes manufacturing costs, and that costs representing injuries and demolition are not present. Creating a model list requires the user to understand what each model does, as well as how a life-cycle assessment should be performed.

A method to ensure that all the relevant costs in a life-cycle assessment are being accounted for is to use a cost matrix. Figure 3.2 shows a sample cost matrix, with the cost categories forming the axes of the matrix. The cost matrix helps the user visualize what costs are being included by the scenario model list, and see what costs need to be accounted for. Costs that are to be included in the life-cycle assessment are marked with $\mathbf{c_i}$. For example, $\mathbf{c_4}$, the direct cost of hazardous events, represents the cost of building damage. The sample matrix shown here has entries for all available cost models currently existing in Rts. The models developed and implemented as part of the current research primarily address deficiencies in $\mathbf{c_1}$, $\mathbf{c_2}$, and $\mathbf{c_3}$.

	Manufacturing	**Construction**	**Operation**	**Hazardous Events**	**Demolition**
Direct Cost	c_1^*	c_2^*	c_3^*	c_4	c_5
Environment	c_6	c_7	c_8		c_9
Safety				c_{10}	
User Experience					

Figure 3.2 Sample cost matrix using existing Rts cost models. The costs primarily addressed in the current work are labelled with asterisks.

Notice that many of the matrix cells are still not accounted for. Some of these, such as the user experience during construction, are nonsensical entries, while others, such as the environmental impact caused by a hazardous event, have no models available. Additionally, some costs do not fit in the cost matrix, such as maintenance costs, or may occupy multiple cells. Nonetheless, the matrix is effective as a tool to help build a scenario model list. The costs numbered in Figure 3.2 will be used to give context in later sections describing the models, as well as in the parametric studies described in Chapter 4.

Direct construction and manufacturing costs are likely the best-studied costs and are also the ones typically minimized in design. These are the initial costs the owner pays to raise a structure. Generally, this includes the cost of materials, labour, and contractor overheads. Costs such as land purchase cost and permitting fees might also be included in this category. One approach to model these has been to use RSMeans data to formulate expressions to calculate costs. Gill (2017) developed expressions to estimate costs for different building components by applying linear regression to 2011 RSMeans data, a model described in Section 3.4. Another potential method might be to use an API (application programming interface). There are many existing commercial BIM-compatible cost-estimating software that draw on real-time databases, including RSMeans, that may be accessible in Rts using an API. Construction cost models may also be considered suitable for the implementation of additional tasks, such as schedule management or calculation of labour-hours. Section 3.11 describes a new detailed construction cost model which aims to expose influential factors in the sources of direct costs, such as the price of materials, while returning required labour-hours.

Environmental impact, specifically climate change, is another cost that has much study devoted to it. There are already existing software such as the Athena Impact Estimator (The ATHENA Institute, 2013) that can quickly calculate the cradle-to-grave emissions of a product in CO_2-

equivalents. Furthermore, there is existing work to estimate the social cost of pollution, primarily carbon emissions. Nordhaus (2011) estimated the social cost of the impact of CO_2 release on global human health and the resulting economic loss. The social cost of all pollution in Canada alone was estimated to be over 40 billion CAD (International Institute for Sustainable Development, 2017), including health impacts, economic losses, and reductions in quality-of-life. Notably, these studies either maintain narrow scopes, or explain the difficulties of costing certain environmental impacts, such as land use. In Rts, SCAR factors (Shindell, 2015) have been used to estimate the social cost of different types of emissions, based on health impacts and global economic loss predictions. Estimates of the embodied energy of construction materials may be obtained from databases such as the ICE (Hammond & Jones, 2008), broken down by energy source. The energy models and social costing model currently existing in Rts are described in Section 3.5.

Other major costs typically associated with life-cycle costs and optimization are direct operating and maintenance costs. Operation activities can comprise the majority of life-cycle costs, both financially and in greenhouse gas emissions (Faludi, Lepech, & Loisos, 2012). The financial costs are accumulated and converted to present worth using economic theory, and the damage caused by emissions is calculated using SCAR factors. Operating energy use may be estimated from statistics, or calculated by specific programs, such as eQuest (James J. Hirsch & Associates, 2016). A new maintenance model for concrete components is described in Section 3.12, based on current research on the deterioration of reinforced concrete.

Demolition cost models are also included in Rts, describing the costs and impacts of recycled material and landfilling. They have relatively little impact on the total life-cycle cost of the building due to the large discounting factor applied to them after many years of a building's design life. Noticeably, the example in the parametric study described in Chapter 4 indicates that recycling may lead to negative net demolition costs.

The social cost of casualties may be estimated using the average value of a statistical life (VSL) (Robinson & Hammitt, 2015). The average VSL estimates the benefit of preventing a fatality, or conversely, the cost of a fatality. While it is both controversial and lacking in precision, policy-makers use it nonetheless, such as in health-care and risk management. The HAZUS technical manual (Federal Emergency Management Agency, 2015) studied the cost of casualties based on different casualty states and collapse states. Casualty costs are also modelled in Rts (Gill, 2017) but are not discussed in this thesis.

User-experience costs, such as aesthetics or comfort, were also considered. However, very little research exists in this field. The IISD (2017) estimated the cost of noise pollution due to transportation to be between 345 million and 3 billion CAD. Kim, Hong, Jeong, Koo, and Jeong (2016) found that thermal comfort had positive correlation with decreased energy use in an optimization study. This did not lead to any estimates on the cost of thermal comfort, but did indicate that energy use, already a direct and environmental cost, has additional unquantified costs.

Previously, many of the existing models described in the following sections were contained in the class RDetailedBuildingModel. Part of the current work was to develop the model framework described above and extract these models to fit in such a way as to maintain plug-and-play functionality. Further work was done to review these existing models and make changes to address some of the model's weaknesses. Finally, as mentioned previously, new models for construction and preventative maintenance were developed to address major deficiencies in the existing models.

3.4 RGurvinderDirectConstructionCostModel

The existing construction cost model, named after the developer, Gurvinder Gill, returns the total direct cost from both the manufacturing and construction phases of the building life-cycle, using a BIM. This model calculates the costs for $\mathbf{c}_1$ and $\mathbf{c}_2$ in Figure 3.2. The model contains expressions to calculate the construction cost for different components, given their specifications, as well as the parameters used by the costing expressions. The cost of the components is summed together to produce the total cost. Notice that this model only considers the cost of the structure itself, excluding other costs such as the land, non-load-bearing components, or the building systems. This model takes a BIM as its only input and returns a cost response as its only output.

RSMeans data was used to generate these empirical expressions through linear regression, resulting in some model uncertainty which is represented using random variables. Notice that the uncertainty in the cost itself is not accounted for. The random variables for this model are all normal random variables, which in this thesis will be written with the form $N(\mu, \sigma)$ where μ is the mean and σ is the standard deviation.

The construction cost of a circular concrete column is (Gill, 2017)

$$C = \left(\frac{\theta_1}{3.048} h + \frac{\theta_2}{0.41} d + \frac{\theta_3}{27.58 \cdot 10^6} f'_c + \frac{\theta_4}{0.41} \rho d + \varepsilon \right)^3 \tag{3-2}$$

where C is the cost of the component, h is the height in metres, d is the diameter in metres, f'_c is the compressive strength in Pa, ρ is the steel ratio, and $\theta_1 = N(3.01, 0.057)$, $\theta_2 = N(2.67, 0.051)$, $\theta_3 = N(0.76, 0.019)$, $\theta_4 = N(33.06, 0.43)$ and $\varepsilon = N(0, 0.42)$.

The construction cost of a concrete slab is (Gill, 2017)

$$C = \left(\theta_1 l + \theta_2 w + \theta_3 t + \frac{\theta_4}{10^6} f'_c + \theta_5 \rho + \varepsilon \right)^3 \tag{3-3}$$

where l and w are respectively the longer and shorter side lengths in metres, t is the thickness in metres, and $\theta_1 = N(1.15, 0.109)$, $\theta_2 = N(0.925, 0.114)$, $\theta_3 = N(11.51, 1.04)$, $\theta_4 = N(-0.0447, 0.146)$, $\theta_5 = N(359.8, 31.3)$ and $\varepsilon = N(0, 0.8)$.

The construction cost of a timber beam-column component is (Gill, 2017)

$$C = \left(\theta_1 h + \frac{1}{2} \theta_2 \left(w + d \right) + \varepsilon \right)^3 \tag{3-4}$$

where d and w are the cross-sectional dimensions in metres, h is the length in metres, and $\theta_1 = N(1.12, 0.02)$, $\theta_2 = N(13.4, 0.13)$ and $\varepsilon = N(0, 0.16)$.

The construction cost of a CLT panel component is (Gill, 2017)

$$C = \left(\theta_1 l + \theta_2 w + \theta_3 t + \varepsilon \right)^3 \tag{3-5}$$

where l and w are respectively the longer and shorter side lengths in metres, t is the thickness in metres, and $\theta_1 = N(1.34, 0.13)$, $\theta_2 = N(0.104, 0.0007)$, $\theta_3 = N(17.3, 1.46)$ and $\varepsilon = N(0, 0.43)$.

The construction cost of a W-section steel beam-column component is (Gill, 2017)

$$C = \left(\theta_1 h + \theta_2 d + \varepsilon\right)^3 \tag{3-6}$$

where h is the length in metres, d is the web height in metres, and $\theta_1 = N(1.45, 0.18)$, $\theta_2 = N(13.9, 3.96)$ and $\varepsilon = N(0, 0.489)$.

Finally, the construction cost of a corrugated steel plate component is (Gill, 2017)

$$C = \left(\theta_1 l + \theta_2 w + \theta_3 t + \varepsilon\right)^3 \tag{3-7}$$

where l and w are respectively the longer and shorter side lengths in metres, t is the thickness in metres, and $\theta_1 = N(0.61, 0.45)$, $\theta_2 = N(0.741, 0.34)$, $\theta_3 = N(36, 4.72)$ and $\varepsilon = N(0, 1.4)$.

A review of the model notes that not all component classes are addressed by the above equations; hence this model should be used with care, as components that are not accounted for will contribute no cost. Additionally, the results should be adjusted to account for inflation since 2011, when the data that was used to generate these equations was collected.

3.5 RShindellEnvironmentalCostOfEnergyModel

The RShindellEnvironmentalCostOfEnergyModel, also developed by Gill (2017), takes energy use responses as inputs and returns the cost of that energy use. This model calculates the costs for $\mathbf{c_6}$ to $\mathbf{c_9}$ in Figure 3.2. It functions in conjunction with energy use models, which calculate the energy use of different building processes. Some of these models in turn require more external inputs, for example, the construction energy model requires the total construction labour-hours to evaluate. The energy use inputs are separated by the type of energy source that is used. For clarity, a portion of the input line for an environmental cost model is shown below.

```
RShindellEnvironmentalCostOfEnergyModel
|ObjectName: SeadonsModel
|JouleCoalList: theManufacturingEnergyModelJouleCoalResponse;
theTransportationEnergyModelJouleCoalResponse;
|JouleDieselList: theManufacturingEnergyModelJouleDieselResponse;
theTransportationEnergyModelJouleDieselResponse
```

The attribute JouleCoalList takes multiple responses, which are in turn responses from other models. The models "theManufacturingEnergyModel" and "theTransportationEnergyModel" must each also return responses with the values for energy use in the form of coal and diesel consumption. Energy use models should be carefully studied to assess which types of responses they return, to be properly input into the environmental cost model.

The Shindell cost model uses social cost of atmospheric release conversion factors to convert energy use into cost (Shindell, 2015). The energy use of building processes comes from various sources, such as the inventory of carbon and energy.

The expressions for the environmental cost of consuming different fuels is given as (Gill, 2017)

$$C_i = \frac{F_i E_i}{D_i} \tag{3-8}$$

where C_i is the cost of fuel i, F_i is the "fuel-to-cost conversion factor" in dollars per cubic metre, D_i is the energy density in joules per cubic metre, and E_i is the energy use in fuel type i in joules. The parameters are given in Table 3.2. Notably, some of the values in this model do not precisely follow the definitions of F and D, such as electricity, which cannot be measured in volume. Specifically, coal, electricity and natural gas have been assigned values such that they produce the appropriate results when used in equation 3-8.

The Shindell cost model accepts seven different fuel types for energy use: coal, diesel, natural gas, LPG (liquefied petroleum gas), gasoline, electricity, and fuel oil. The energy use models pass sets of responses with the energy required for different processes, separated by fuel type.

Table 3.2 Values of cost conversion factors and energy densities (Shindell, 2015).

Fuel Type	$\boldsymbol{F}$ (\$/m^3)	$\boldsymbol{D}$ (J/m^3)
Coal	N(6.67 e-8, 1.33 e-8)	1
Diesel	N(1.268, 0.25)	35 800 000
Electricity	N(40.05, 8)	1 000 000 000
Fuel Oil	N(1.268, 0.25)	34 800 000
Gasoline	N(1.0039, 0.2)	34 200 000
LPG	N(0.904, 0.18)	26 000 000
Natural Gas	N(3.06 e-8, 7.12 e-9)	1

While this model uses the fuel type to determine the environmental cost of energy use, Shindell actually studied the social cost of releasing different types of atmospheric pollutants (2015). The cost of fuel use was included in the referenced paper as a conclusion regarding the net emissions of various industrial sectors. Hence, the existing model's use of the SCAR factors is a large approximation of the actual research results. Additionally, Shindell assumes certain discounting rates to account for future loss; however, this is not accounted for in the existing Rts model.

3.6 REnergyUseInManufacturingModel

The energy used in manufacturing construction materials (Gill, 2017) is calculated using data from the inventory of carbon and energy (Hammond & Jones, 2008). In conjunction with the Shindell environmental cost model, this model calculates the cost for $\mathbf{c_6}$ in Figure 3.2. The only input required by the manufacturing energy model is the BIM; the only outputs returned are the energy use responses.

The general expression for energy use in manufacturing is given as (Gill, 2017)

$$E_i = \sum_j M_j I_j P_{ij} \tag{3-9}$$

where M_j is the mass of construction material j in kg, I is the manufacturing energy intensity in joules per kg, and P_{ij} is the portion of energy sourced from fuel type i. The parameter values are given in Table 3.3. Fuels that are not shown are not used in the manufacturing of these materials. Note that the equation above does not account for non-energy-use sources of emissions, which account for a large portion of the emissions in concrete manufacturing.

Table 3.3 Values of manufacturing intensities and fuel-type portions (Hammond & Jones, 2008).

Fuel Type	Concrete	Steel	Timber
I (J/kg)	*N*(950 000, 95 000)	*N*(36400000, 3640000)	*N*(8500000, 850000)
P_{coal}	0.471	0.17	0
$P_{electricity}$	0.344	0.5	0.242
$P_{fueloil}$	0.154	0	0.728
$P_{naturalgas}$	0.031	0.33	0.03

3.7 REnergyUseInConstructionModel

The energy used in construction is given by the REnergyUseInConstructionModel (Gill, 2017). This model takes the total construction labour-hours as an input, as well as the BIM; the only outputs are the energy use responses. In conjunction with the Shindell environmental cost model, this model calculates part of the cost for $\mathbf{c}_7$ in Figure 3.2. The energy used in the construction itself is modelled to be only the energy drawn by heavy machinery used in construction, such as cranes or excavators. This energy use is modelled as (Gill, 2017)

$$E_{diesel} = \alpha It \tag{3-10}$$

where the fuel source is diesel, α is the heavy machinery use ratio, t is the total construction labour-hours, and I is the machinery's energy usage intensity in joules per hour, given by I = N(268000000, 53600000). This model is a statistical approximation of heavy machinery use, which will vary between buildings. The development of a construction schedule management model would lead to much better estimates of the energy demand from this model.

Table 3.4 Ratios of heavy machinery use by builing type.

Building Type	Value of α
Timber high-rise	0.1
Concrete high-rise	0.3
Steel high-rise	0.3
Timber low-rise	0.05
Concrete low-rise	0.1
Steel low-rise	0.1

3.8 REnergyUseInTransportationModel

In conjunction with the Shindell environmental cost model, this model calculates part of the cost for **c7** in Figure 3.2. The energy used in transporting materials to the worksite is given by (Gill, 2017)

$$E_{diesel} = \left(\frac{1}{2} V_{concrete} d_{concrete} + V_{steel} d_{steel} + \frac{1}{3} V_{wood} d_{wood} \right) I \qquad (3\text{-}11)$$

where V_i is the building's volume of material i in cubic metres, d_i is the round-trip distance from the building site to the material source, and the vehicle energy usage is $I = N(1000, 100)$ in joules per metre. This model takes locations of material and worker sources as inputs to calculate the distance to the building site.

Transporting workers is assumed to happen by three possible means: rapid transit, public bus, or car. Each of these use a different energy source, and the usage of energy is modelled as (Gill, 2017)

$$E_{diesel} = 0.2 d_{wo} \frac{t_{total}}{t_{day}} I_{bus} \tag{3-12}$$

$$E_{electricity} = 0.3 d_{wo} \frac{t_{total}}{t_{day}} I_{mrt} \tag{3-13}$$

$$E_{gasoline} = 0.5 d_{wo} \frac{t_{total}}{t_{day}} I_{car} \tag{3-14}$$

where d_{wo} is the round-trip distance for workers to reach the building site, t_{total} is the total labour-hours for construction, t_{day} is the length of a work day in hours, and I_k is the vehicle energy usage in joules per metre, modelled as $I_{bus} = N(920,92)$, $I_{mrt} = N(390,39)$, and $I_{car} = N(2730,273)$.

Previously, this model used fixed distances to material source locations, and fixed ratios for the transportation of workers using different means of commute. One of the changes made as part of the current work to this model was implementing the use of source locations.

3.9 REnergyUseInOperationModel

The operating energy model, in addition to returning the fuel-demand responses used by the environmental costing model, also returns the direct utility cost to the scenario model. This model calculates the cost for **c_3** in Figure 3.2, as well as providing input to the environmental cost model to calculate **c_8**. The energy used during a building's operation is evaluated in regular intervals, and the fuel-demands are modelled as

$$E_{electricity} = 0.383E'\Delta t \tag{3-15}$$

$$E_{naturalgas} = 0.617E'\Delta t \tag{3-16}$$

where E' is the daily energy use in joules per day, and Δt is the time since the last evaluation, in days. The daily energy use depends on many factors, such as the building's location and windows and shading, is not modelled in Rts and needs to be input by the user. The direct cost of the energy use is modelled as

$$C = (0.383C'_{electricity} + 0.617C'_{naturalgas})E'\Delta t \tag{3-17}$$

where C'_i is the price per joule of energy source i, which varies by the building's location. The current prices are \$12.43 per kWh of electricity and \$6.662 per GJ of natural gas. The proportions of energy usage type are given by Natural Resources Canada (Natural Resources Canada, 2017).

The current work aimed to address some of the weaknesses in this existing model. In addition to the costs of natural gas and electricity, which were given new values based on Vancouver prices in 2018, this model accepts a value for the daily energy usage. The default value given by the model is the average for a Canadian house; however, external study is required to obtain an accurate estimate of daily energy use. As such the current model still does not account for any deviations, such as the size of the home or the effectiveness of the insulation. The technical manual for eQuest (James J. Hirsch & Associates, 2016) includes the expressions which are implemented in the program to calculate energy usage. Either these or an API could be used to improve the estimation of energy usage in Rts.

3.10 RGurvinderDemolitionCostModel

This cost model returns the sum of costs occurring during the demolition phase, as well as some energy use responses. Direct costs are the cost of landfilling, and the profit made from selling recycled material. Energy use or savings result from recycling materials and transporting waste material to the landfill. This model calculates the cost for $\mathbf{c_5}$ in Figure 3.2, as well as providing input to the environmental cost model to calculate $\mathbf{c_9}$.

The direct cost is given as (Gill, 2017)

$$C = C'_{landfill} \sum_i m_i \left(1 - r_{recycle,i}\right) - \sum_i m_i r_{recycle,i} C'_i \tag{3-18}$$

where $C'_{landfill}$ is the cost of landfilling in dollars per kilogram, m_i is the total building mass of construction material i, $r_{recycle}$ is the recycling rate of each material, and C'_i is the market price for materials. The parameters are given in Table 3.5. Note that C'_i should be adjusted by the user to suit the actual circumstances of a simulation. The last column contains information used for calculating the environmental cost of demolition.

Table 3.5 Parameters for calculating the cost of demolition (Gill, 2017).

Material	$r_{recycle}$	C'	f_E
Concrete	0.85	$N(0.06, 0.009)$	0.5
Steel	0.98	$N(2.0, 0.3)$	0.3
Wood	0.98	$N(0.5, 0.75)$	0.6

For coal, fuel oil, electricity, and natural gas, the energy used or saved in demolition is modelled as (Gill, 2017)

$$E_i = \sum_j m_j r_{recycle,j} \left(1 - f_{E,j}\right) I_j P_{ij} \tag{3-19}$$

where E_i is the energy use in fuel type i in joules, m_j is the total mass of construction material j in kilograms, and $r_{recycle}$, I, and P are defined as above in equations 3-9 and 3-18. f_E is the fraction of energy used to make construction materials from recycled material, relative to that which is normally required, given above in Table 3.5.

3.11 RSeadonDirectConstructionCostModel and RDirectCostOfMaterialsModel

A new model to calculate the direct costs of manufacturing and construction of concrete components was developed in the current work, and is described here. This model attempts to add transparency to the sources of costs to allow the user to adjust the costing parameters based on available market information. Additionally, a prediction of the total labour-hours necessary for construction is also produced. The new cost model is based on the RSMeans Estimating Handbook 3rd Edition (Means Engineering Staff, 2009) and RSMeans 2018 data. This model primarily calculates the cost for $\mathbf{c_2}$ in Figure 3.2. A simple material cost model, RDirectCostOfMaterialsModel, the expressions for which are provided in this section, calculates the costs for $\mathbf{c}_1$.

There exist many commercial cost-estimating software, such as BuilderTrend or Innovaya. While it could be possible to for Rts to use an application programming interface (API) to take advantage of one of these, Rts is intended to be a standalone program. Gill (2017) previously developed cost models for many classes of components by applying linear regression techniques to RSMeans costing data.

Construction of concrete components typically involves five steps: formwork, placing reinforcement, pouring, curing, and stripping. Each step contributes to the total cost through the cost of materials, and the costs of labour and equipment. This model combines the costs for formwork and stripping, as provided in RSMeans. Curing does not contribute any costs but may be necessary to consider in the future for schedule management models.

The general expressions for the six remaining costs are given in Table 3.6, with all costs in 2018 USD, where V = volume, A_S = surface area, ρ = reinforcement ratio, and C_i = total cost for item i. The cost items have been separated by construction phase, and by whether they are the price of the raw materials, or the cost of the construction process itself.

The expressions under the "Materials" column of Table 3.6 are placed in the materials cost model, while the "Labour & Equipment" items are placed in this model. The costing parameters above are described in

Table 3.7. The given values are valid for 2018 construction, averaged over the US. If available,

the user should modify the cost parameters, such as the cost of carpenters, to reflect the actual circumstances of the project.

Table 3.6 Expressions for concrete component manufacturing and construction costs.

	Materials	**Labour & Equipment**
Formwork	$C_{forms} = 1.1C'_{forms} f_{forms} A_S$	$C_{carpenters} = C'_{carpenters} t_{forms} A_S$
Reinforcement	$C_{steel} = 1.1C'_{steel} \rho V$	$C_{rodmen} = C'_{rodmen} t_{steel} \rho V$
Pouring	$C_{concrete} = 1.1C'_{concrete} V$	$C_{pouring} = C'_{pouring} t_{pouring} V$

Table 3.7 Parameters for concrete component construction cost estimating.

Parameter	**Description**	**Value**	**Unit**
C'_{forms}	Volumetric cost of form material	370	$/m^3
f_{forms}	Ratio of form volume to component surface area	See Table 3.8	m
$C'_{carpenters}$	Hourly cost of carpenters	71.59	$/h
t_{forms}	Hours to build, erect and strip forms	1.9	h/m^2
C'_{steel}	Volumetric cost of reinforcing steel	8453	$/m^3
C'_{rodmen}	Hourly cost of rodmen	83.70	$/h
t_{steel}	Hours to place reinforcing steel	189.3	h/m^3
$C'_{concrete}$	Volumetric cost of concrete	See equation 3-23	$/m^3
$C'_{pouring}$	Hourly cost of pouring crew and pumping equipment	79.04	$/h
$t_{pouring}$	Hours to pour concrete	See Table 3.10	h/m^3

Table 3.8 Values of ratios of form volume to component surface area.

Component	Value of f_{forms} (m)
Rectangular beams and columns	0.0762
Circular columns	See equation 3-20
Slabs	0.0508
Walls	0.0635

Table 3.9 shows the construction time for different types of forms. Notice that there is slightly correlation between t_{forms} and f_{forms}, meaning the components requiring more form material also require more construction time.

Table 3.9 Time to build forms for different components.

Component	Value of t_{forms} (h/m^2)
Rectangular beams and columns	1.9
Circular beams and columns	See equation 3-21
Slabs	1.0
Walls	1.83

Circular forms are typically pre-fabricated from paperboard or fibreglass. The material cost for circular forms is given by the empirical expression

$$C_{forms} = 1.1h(71.8d^2 + 6.45) \tag{3-20}$$

The time required to erect circular forms is given by

$$C_{carpenters} = C'_{carpenters}\, h(0.335d + 0.6) \tag{3-21}$$

where d = diameter in metres, and h = column height in metres.

Table 3.10 shows the time required to pour forms for different components. Columns of both cross-section types as well as beams share the same rate of pouring, as per RSMeans.

Table 3.10 Rates of pouring concrete for different components.

Component	Value of $t_{pouring}$ (h/m³)
Beams and columns	See equation 3-23
Slabs	0.5
Walls	0.65

The rate of pouring varies with the size of the component. For beams and columns, the time rate is given as

$$t_{pouring} = \frac{1}{12x + 2.35} \tag{3-22}$$

where x represents the diameter or larger cross-sectional dimension in metres.

The price of concrete roughly varies with the compressive strength f_c, and is given as

$$C'_{concrete} = 0.834 f'_c + 142.9 \tag{3-23}$$

where f'_c is given in MPa.

3.12 Preventative Maintenance Model

This new model calculates the cost of maintenance of concrete building components over a building's lifetime. As mentioned above, operation and maintenance costs can contribute to the majority of a building's total life-cycle cost (Faludi et al., 2012). While Gill (2017) implemented a simple model to calculate the operating energy costs of a building, no maintenance cost model was implemented in Rts. This section describes the development of the model that addresses this need.

The three major types of construction materials are wood, steel, and concrete. All three suffer deterioration in different forms; wood suffers from decay, steel from rust, and concrete from various forms of degradation. Melchers (2003) noted that the corrosion of structural steel components is confined to older structures lacking in corrosion protection, and that there is a lack of research in this area. The decay of wood components is even less understood, with very little literature available. Thus, only the degradation of concrete components is modelled here.

Degradation of reinforced concrete can occur due to corrosion of reinforcing steel, swelling due to alkali aggregate reactions, and several other rarer causes. Of these, the corrosion of reinforcing steel is the best understood. Additionally, the rusting of steel causes cover concrete to spall, further accelerating the degradation process, making it a significant threat to the durability of concrete structures. For these reasons, concrete degradation due to corrosion of reinforcing steel will be the only form of degradation studied in this model.

Rusting naturally occurs on the surface of iron in the presence of water and oxygen. However, in reinforced concrete, the extremely alkaline environment of the concrete causes a thin metal hydroxide layer to form on the surface of the reinforcing steel. This layer protects the steel from corrosion, a phenomenon known as passivation, that occurs if the high pH of the environment is maintained.

Nonetheless, there are two ways reinforcing steel can corrode inside the concrete environment (Zhao & Jin, 2016). One is chloride-induced corrosion, where chloride ions cause de-passivation and allow the steel to rust, which is prevalent in concrete components near the surface of seawater. The other is carbonatation, commonly called carbonation by engineers, in which atmospheric carbon dioxide reacts with water to form carbonic acid. This acid gradually lowers the pH of the concrete environment, eventually leading to de-passivation and corrosion.

Tutti's curve, shown in Figure 3.3, shows the progression of the deterioration of reinforcing steel over time. During the initiation phase, carbonation causes the concrete environment to lose pH, though the strength of the steel is not affected. Eventually, the pH drops enough for corrosion to begin, signalling the start of the propagation phase. The steel begins to lose cross-sectional area, until the loss of strength exceeds acceptable levels, and the service life of the component is exhausted.

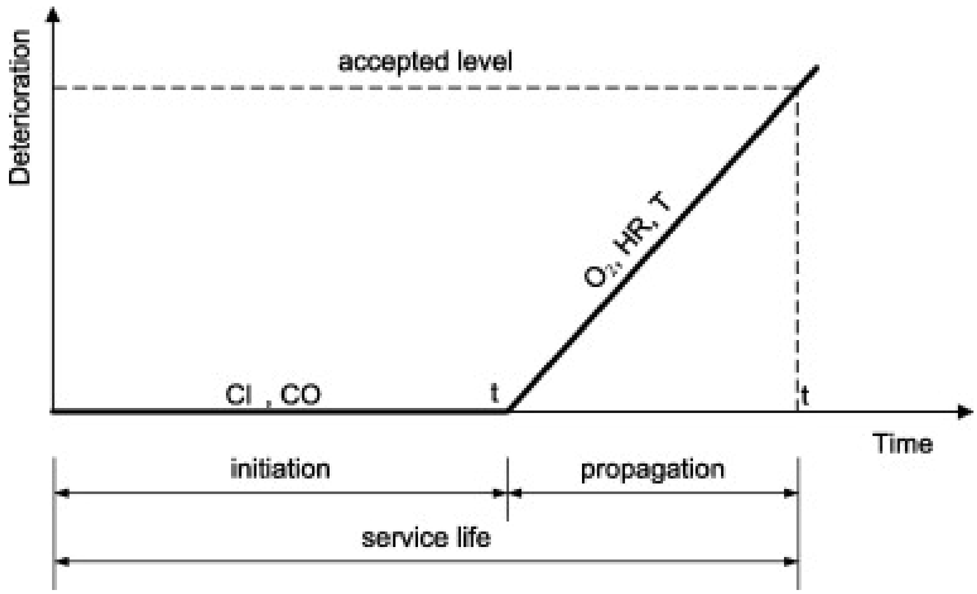

Figure 3.3 Tutti's curve, describing carbonation and corrosion of reinforced concrete.

While the propagation phase is an important research topic (Zhao & Jin, 2016), the necessary replacement of reinforcing steel represents a time-consuming and costly task for building owners. Not maintaining the structure, and allowing the structural steel to corrode, is expected to produce even greater life-cycle costs. Furthermore, the modelling of corrosion propagation is complex and poorly studied. Thus, this model assumes that the concrete cover is always replaced near the end of the initiation phase, and only models the initiation phase. Thus it also does not model effects such as spalling due to rusting, or deterioration of the reinforcing steel.

Most carbonation models follow Fick's first law of diffusion (Monteiro et al., 2012; Torres, Correa, Castaño, & Echeverría, 2017). The general form for such models is given in equation 3-24, where x is the depth of penetration of carbonation, t is the duration of carbonation, and K is the carbonation coefficient.

$$x = K\sqrt{t} \tag{3-24}$$

However, Monteiro et al. (2012) point out that most studies include an enormous range of factors, such as CaOH content and atmospheric carbon dioxide and oxygen levels. These are impractical for designers to measure and result in excessively complex models crippled with large amounts of uncertainty.

Monteiro et al. (2012) developed a simple statistical model with *K* varying only with concrete strength. While only valid for unpainted exposed concrete, it captures the worst-case scenario for concrete components removed from marine environments. The derived expression for *K* is given in equation 3-25, where *K* is the carbonation coefficient in mm/y$^{0.5}$ and f_{cm} is the mean compressive strength of the concrete in MPa.

$$K = 847\, f_{cm}^{\;-1.435} \tag{3-25}$$

Given the mean compressive concrete strength for a concrete component and the component's cover depth, the duration of the initiation phase may be solved for from the above equations.

The preventative maintenance model developed here then designates points in a component's lifetime at which it will be required to undergo maintenance. These points are separated by a duration of time equal to the estimated carbonation initiation phase of the component's cover concrete. Note that the mean compressive strength of a component is not typically given, and that the above expressions must accept the nominal compressive strength instead. This provides additional conservativism; however, the loss of accuracy indicates that the relationship between mean and nominal strength requires further study.

Upon reaching a maintenance point in a component's life-cycle, the component's cover concrete is replaced. The cost of replacing the cover concrete is approximated in equation 3-26, where $C_{concrete}$ is the total cost, d_{cover} is the component's concrete cover's depth, $C'_{concrete}$ is the volumetric price of concrete, and A_S is the surface area of the component.

$$C_{concrete} = C'_{concrete} A_S d_{cover} \tag{3-26}$$

Chapter 4: Parametric Study

This chapter describes and discusses the results of a parametric study that was performed using Rts. Parameters were changed, and the results were examined to understand how each parameter influenced the life-cycle cost. Conclusions were made based on these results regarding the accuracy of the existing models, as well as observations regarding the nature of some of the costs. Some suggestions on future work are made in Chapter 5 based on the results found here.

4.1 Study Background

The study was performed on an example building imported from an IFC file. The complete Rts input file may be found in Appendix A, with explanatory annotations. A 3D render of the example building in the Rts interface is shown in Figure 4.1. The structure consists of circular concrete columns and a concrete slab roof. Non-structural components, such as non-load-bearing walls, are not modelled. The structure's specifications are as summarized as follows:

- Circular concrete columns: 100 mm diameter, 2900 mm height, 2% reinforcement ratio
- Concrete slab roof: 4300 mm x 6700 mm, 102 mm thickness, 3% reinforcement ratio

The costs that are included in this study are the direct construction cost, the environmental costs, the cost of materials used in building maintenance, the cost of operations, and the cost of demolition. The environmental costs account for energy used in manufacturing materials, transportation of materials and workers, construction processes, demolition, and operation. These include all costs included in the cost matrix in Figure 3.2, except for the costs relating to hazardous events, and in addition to the preventative maintenance model.

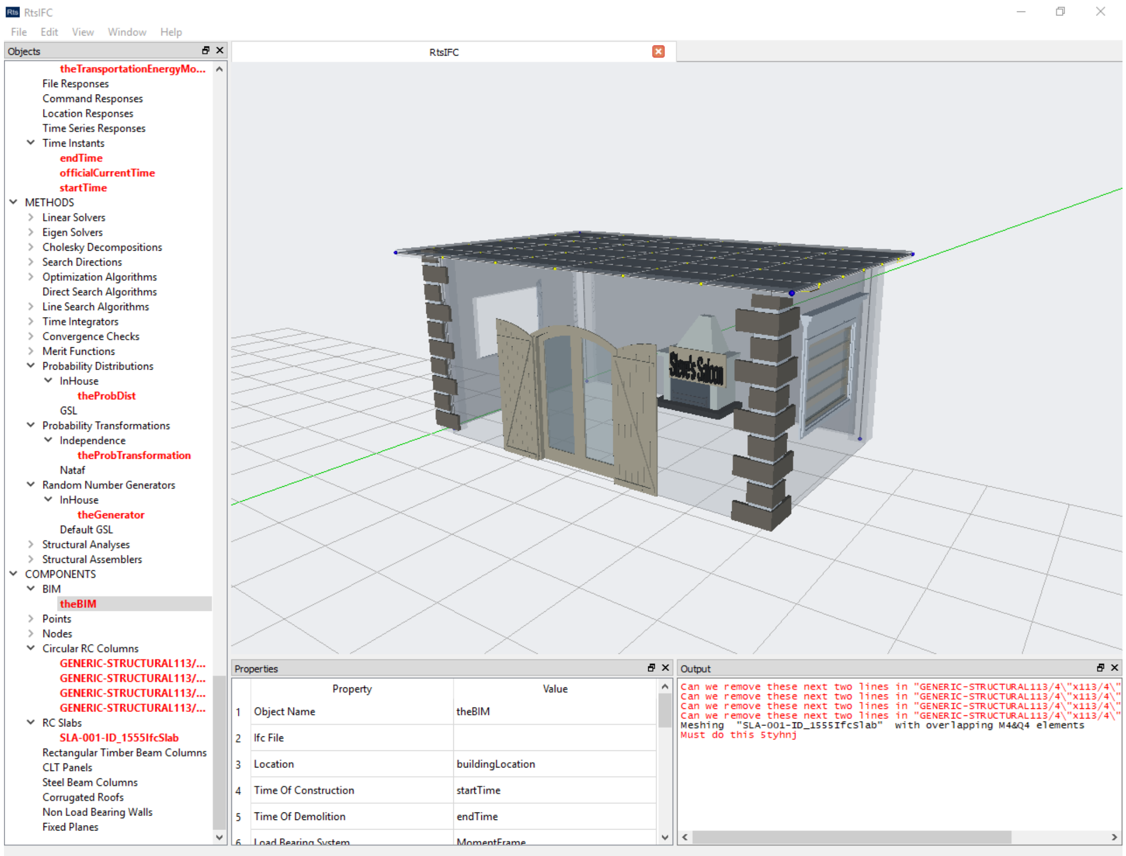

Figure 4.1 Screenshot showing 3D render of the example building in Rts interface.

The model flowchart that was used in this study is shown in Figure 4.2. In this set-up, the material cost model, mentioned in Section 3.11, calculates the cost of construction materials. Also, while not shown here, the transportation and construction energy models take predictions of the total labour-hours from the construction cost model, as one of the advantages of the new construction cost model. Note also that the BIM and components are not included in this figure.

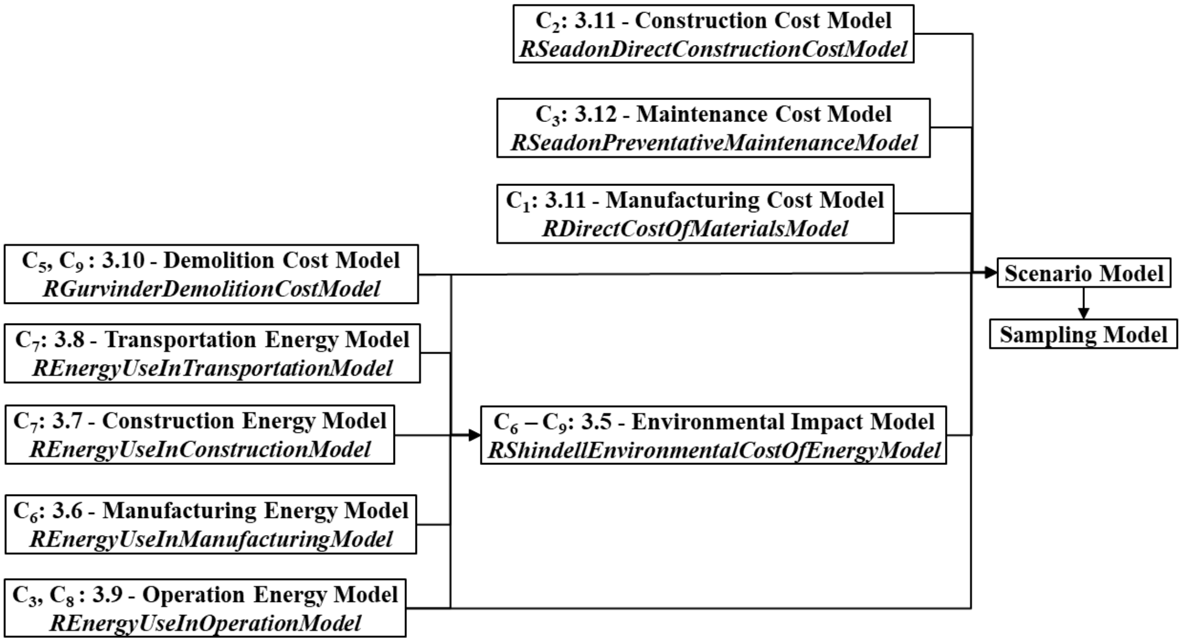

Figure 4.2 Model flowchart used in the parametric study. The model class names are shown in italics; the cost matrix cell number and section number in this thesis are given for reference.

The hazard models have also been excluded in this study. The absence of loads, and the subsequent lack of casualty costs, presents a serious issue that does not allow for optimization in this study. As such, this study will only be focussed on observing the effects of varying parameters from the initial values given above or in the relevant models. Additionally, while most of the costs studied here are subject to uncertainty and randomness, only the mean of the results obtained from Rts are used in the following discussions.

4.2 Building Life-Cycle Cost Contributors

The first objective was to determine cost contributions from the different cost models. To do this, each of the six models passing a response directly to the scenario model is run with the scenario model in isolation. These six models were the manufacturing cost model, the construction cost model, the environmental impact cost model, the operation energy model, the maintenance model, and the demolition cost model. Figure 4.3 shows the results of this analysis. As in Figure 4.2, the material cost is also referred to as the manufacturing cost.

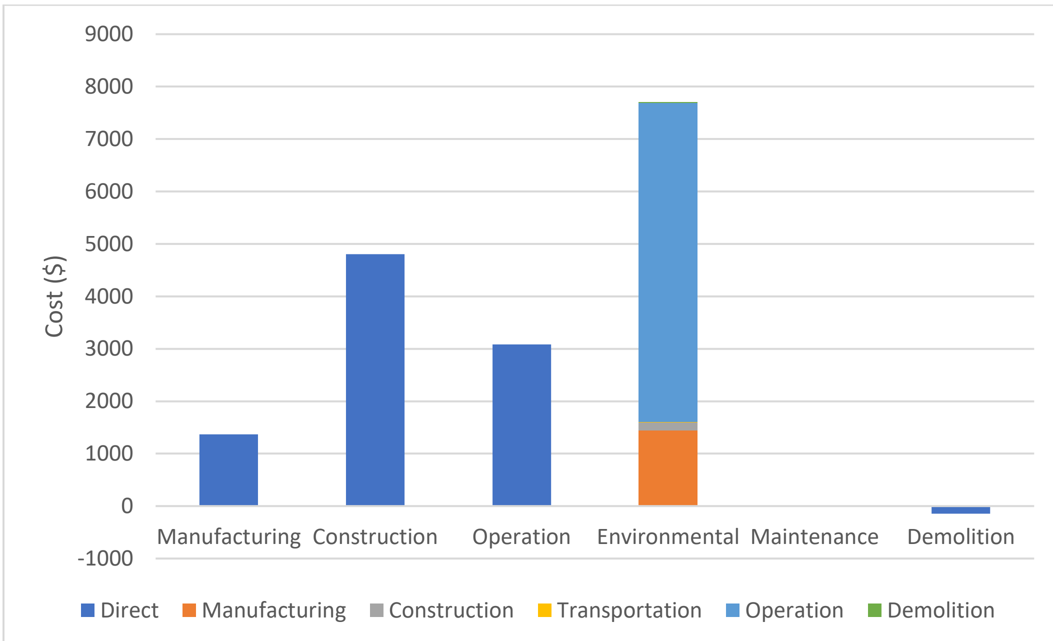

Figure 4.3 Life-cycle cost contributions from different models.

To better understand the environmental impact cost, the four contributing models were each evaluated in isolation with the environmental impact model. The “Environmental” column in Figure 4.3 also indicates the contributions of energy use from different models, detailed in the legend.

The results for the direct costs agree with the literature mentioned in Chapter 3 (Islam et al., 2015), with the operation costs contributing to 33% of the total direct cost. However, as noted in Section 4.1, non-structural component costs are not included. These may include the costs of land purchase, non-load-bearing walls, utility systems, and furnishings. As such, the actual construction cost for the buildings will be much higher. Additionally, the daily energy usage was calculated using the national average per-area energy intensity (Natural Resources Canada, n.d.). However, the sample building is much smaller than the average buildings, resulting in a higher surface-area-to-volume ratio. This would cause the building's energy efficiency to be lower than average, resulting in higher daily energy use than estimated. The cost of materials, specifically steel and concrete, contribute to 22% of the initial direct costs, slightly lower than the prediction of 30% (Means Engineering Staff, 2009).

Notably, the environmental cost contributes the largest share of the total cost, at 45%. Additionally, the environmental impact of operational energy use contributes to 79% of that cost, or 36% of the total cost. This may be reasoned by comparing the environmental cost of energy use to the direct price. For example, BC Hydro charges 0.1243 CAD per kilowatt-hour of electricity, while the estimated environmental cost of electricity use is 40.05 USD per gigajoule, or 0.1442 per kilowatt-hour. Hence, the resulting environmental cost is higher than the corresponding direct cost for operational energy use.

Also notice that the maintenance cost is negligible; this will be discussed further in Section 4.4. The demolition cost is negative due to recycling returns; however, because of discounting it is also negligible compared to the other life-cycle costs.

4.3 Building Design Life and Discount Rate

Two of the most important variables studied were the building design life, and the selected discounting rate. These were selected due to their influence on the total life-cycle cost, and because they reflect the impact of decisions relating to a building's replacement.

The following results were based off a 50-year life-cycle and a discount rate of 5%. Figure 4.4 shows the variation of total life-cycle cost with building design life, up to 100 years. With a design life of zero years, the total cost is $8000. This represents the difference between the initial costs and the demolition-associated costs. Initial costs refer to all costs associated with the manufacturing and construction phases of the building, or, referencing Figure 3.2, equals $\mathbf{c_1} + \mathbf{c_2} + \mathbf{c_6} + \mathbf{c_7}$. The total cost increases with the design life, as the costs of operation in intermediate years are added. Notice that the increase in cost decreases with each additional year of design life; for example, extending a building's design life from 40 to 60 years increases the total cost by less than $2000. This is because the cost contributed by years of operation far in the future are heavily discounted.

While it is impossible to predict what technological advances will be made in 40 years, this does have some significance in decision-making concerning construction of new buildings. For example, the construction cost of a building contributes most of the total life-cycle cost of a building, so buildings with longer lives cost less per year than ones with shorter lives. Hence, the planning of new construction should aim to keep buildings in service for long periods of time, as opposed to frequently demolishing and re-constructing new buildings.

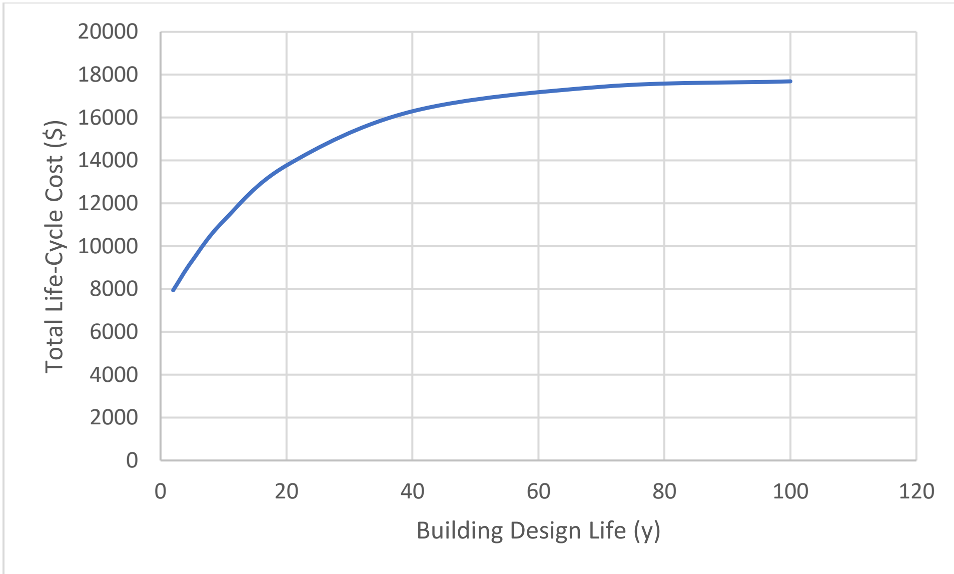

Figure 4.4 Variation of total life-cycle cost with building design life with 5% discounting.

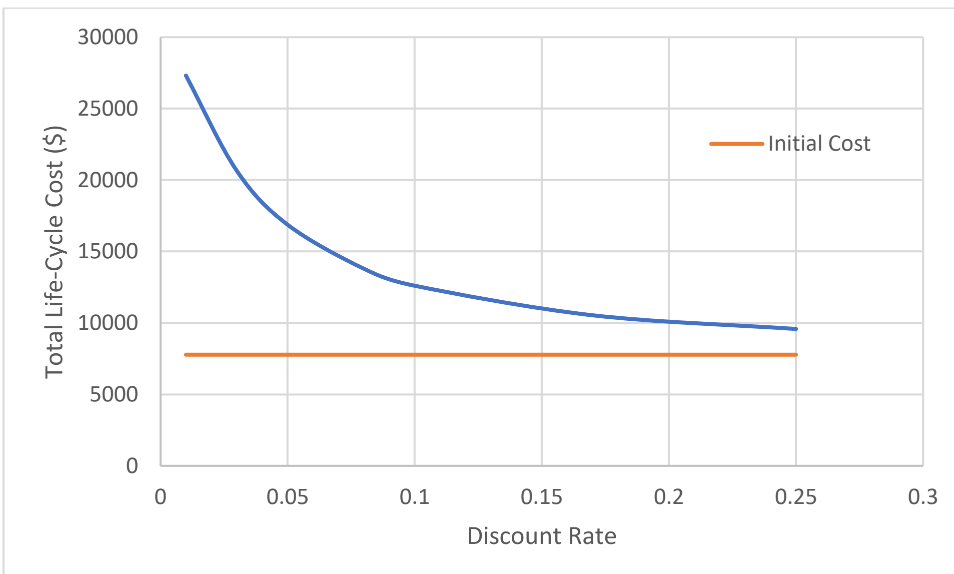

Figure 4.5 Variation of total life-cycle cost with discount rate given a 50-year design life.

Figure 4.5 shows the effect of varying the selected discounting rate. A higher discounting rate causes costs later in the building's life to be devaluated, resulting in a lower total cost. The total initial cost is included for reference. As mentioned in Chapter 3, the selection of a discount rate is a difficult part of life-cycle costing, with significant implications. Discount rates under 1% result in total costs that exceed $25000, while a discount rate of 6% leads to a total cost of only $15000.

4.4 Concrete Cover Depth

The total cost was observed while the concrete cover depth of the circular columns was varied. As the cover depth was varied, the column diameter was adjusted to keep the confined concrete diameter constant. The results are shown in Figure 4.6. The initial column diameter was 100 mm with a cover depth of 30 mm, and a fixed confined concrete diameter of 40 mm.

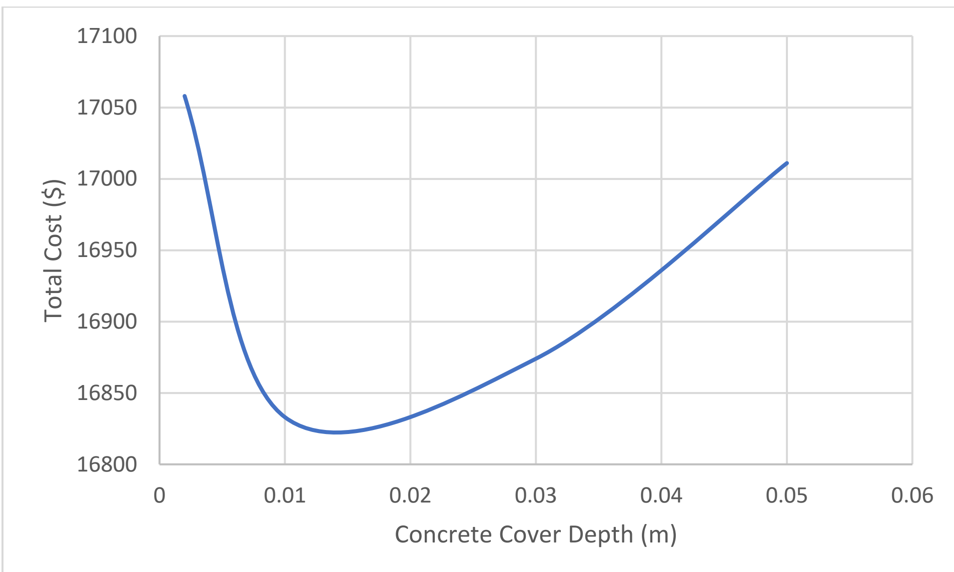

Figure 4.6 Variation of total life-cycle cost with concrete cover depth.

It is observed that an optimum cover depth exists, at approximately 15 mm in this scenario, that results in the lowest total cost. The results of tests with a smaller concrete cover depth showed that the cover was being replaced more frequently. Though each concrete cover replacement costs less, the increased frequency of replacement results in an overall increase in cost.

Increasing the cover depth above the optimum causes the concrete cover to be replaced less frequently. However, the building's design life limits the extent of this benefit. For example, a given column's concrete cover only needs to be replaced once, after 30 years of its 50-year life-cycle. Increasing the concrete cover depth to require a 40-year replacement period does not lower the number of times replacement is required, as one replacement is still necessary. Additionally, as the number of replacements decrease, the column construction cost and cover replacement cost increase, resulting in an overall increase in cost.

The Cement Association of Canada (n.d.) recommends 40 mm cover for exterior columns, much higher than the optimum observed in Figure 4.6. However, it should be noted that the maintenance cost model, as described in Section 3.12, only considers the cost of the concrete material for the replacement. It does not account for the labour costs, nor the indirect costs of stopping business for the repairs. It was seen in Section 4.2 that, for the construction of a building, the material cost is much lower than the labour cost estimated by the construction cost model. Assuming this is also true for cover replacement, the actual cost of each concrete cover replacement is much higher than only the material cost estimated by the maintenance model. This would make it optimal to have very few or even no replacement actions over the building's life-cycle, increasing the optimal concrete cover depth.

4.5 Daily Energy Usage

The average daily energy use of the building was varied, and the total cost was observed; the results are shown in Figure 4.7. The total cost is seen to vary linearly with the daily energy use.

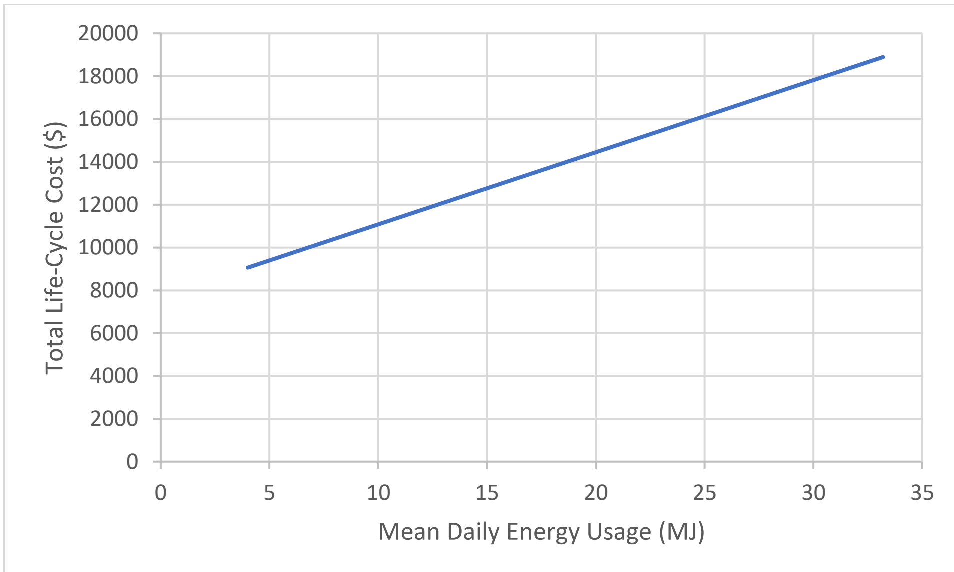

Figure 4.7 Variation of total life-cycle cost with mean daily energy usage.

The range of values of daily energy use selected here is meant to represent the range of energy use of currently existing buildings. Huebner, Shipworth, Hamilton, Chalabi, and Oreszczyn (2016) studied English households and found that the mean annual energy usage has a coefficient-of-variation of 0.073. In this study, the upper limit was selected to include all but the most energy-demanding 0.1% of buildings. Assuming a normal distribution, this indicates an upper bound of 33.2 MJ should be used.

Kurnitski (2013) performed a case study that found that current near-zero-energy-buildings (nZEBs) use one-sixth of the average household's energy usage. As mentioned in Section 4.2, the mean daily energy use is calculated from the average British Columbia energy usage intensity (Natural Resources Canada, n.d.). The mean daily energy use was thus estimated to be 27.2 MJ, assuming average energy use intensity. Using Kurnitski's results, the lower bound for this experiment was selected to be 4 MJ per day.

In agreement with Kurnitski (2013), nZEBs were found to be very economically efficient. It was found that nZEBs may be constructed with relatively small increases to the initial cost, approximately 3-4%. The mean daily energy use was estimated to be 27.2 MJ, with a total life-cycle cost over $16000, for the example building with average energy use intensity. The parametric study shows that an nZEB with the same footprint has a total life-cycle cost of under $10000. Even after accounting for the increase in construction cost, this suggests that the use of green building technologies can be economically efficient.

However, it should be reminded that the daily energy use passed in to the operation energy model is a very rough approximation based on average household intensity. Thus the values derived here should be primarily understood in terms of how they vary with energy usage.

4.6 Environmental Cost of Electricity Use - Hydroelectricity

The SCAR for electricity use is the weighted average of the SCARs for different fuels used to power electricity plants (Gill, 2017). These SCARs were calculated based on US national averages. However, electricity in Vancouver tends to be sourced from hydroelectric dams, which emit comparatively negligible emissions during operation. To simulate this and observe the effect on the total cost of a building, the mean value of F in Table 3.2 for electricity was changed from \$40.05/m^3 to \$4.0/m^3. This represents hydroelectricity use with a 90% decrease in the mean social cost of electricity use, with the assumption that hydroelectricity generation still has some negative impact on the environment. Figure 4.8 shows a comparison of total environmental life-cycle costs between a building using mixed-source electricity and one using hydroelectricity, including error bars at one standard deviation from the mean. The mean environmental cost of a building using hydroelectricity is 39% lower than that of one using mixed-source electricity, representing a cost decrease of \$3000.

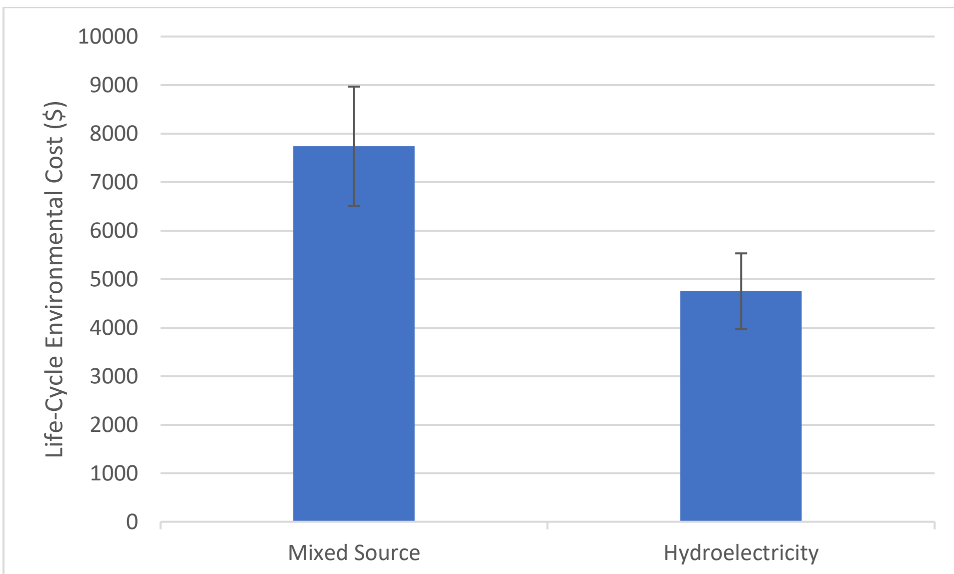

Figure 4.8 Environmental life-cycle cost with mixed-source electricity and hydroelectricity.

Li and Froese (2016) wrote that buildings in Vancouver tend to have relatively low environmental impact due to the use of hydroelectricity during operation. The results in Figure 4.8 confirm that renewable electricity sources do result in buildings with significantly lower environmental impact. Nonetheless, it should be reminded that the Shindell environmental cost model only considers the social cost of atmospheric pollution and its effects on climate change.

Hydroelectric dams affect the environment in other ways, including biodiversity loss and habitat alteration (Fearnside, 2016), that are not costed by the existing model.

4.7 Location of Material Source

Construction materials are typically locally sourced to reduce construction costs, resulting in the low environmental cost of transportation seen in Figure 4.3. However, sometimes material sources may be located further when importing specialized components. Figure 4.9 shows the initial environmental cost of the example building, located in Vancouver, with different material source locations. The initial environmental cost consists of only the environmental costs of manufacturing, construction, and transportation.

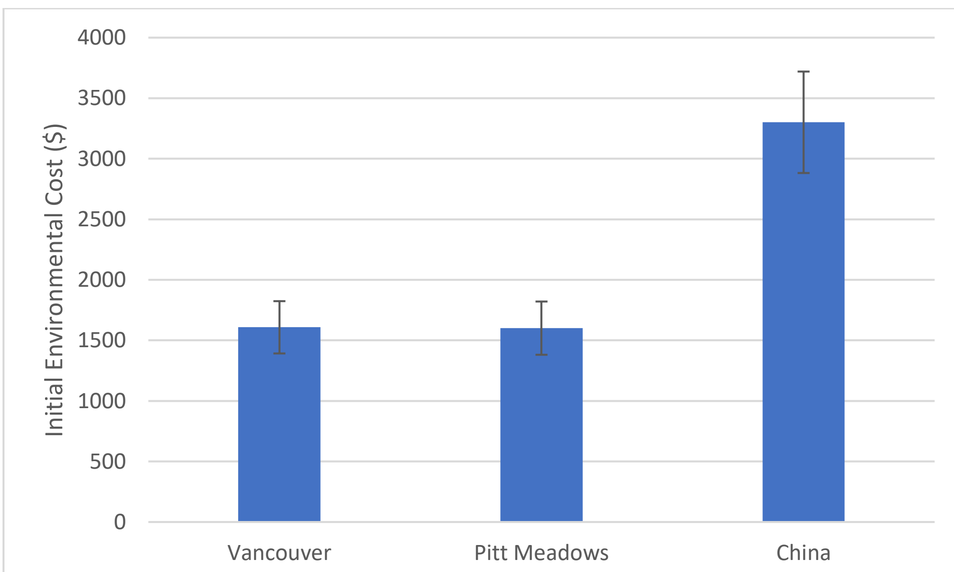

Figure 4.9 Initial environmental cost with different material source locations.

Notably, only drastic changes to the source location result in appreciable differences in the initial environmental cost. The cost increase caused by using a slightly distant location, Pitt

Meadows in this study, is negligible compared to the environmental cost of manufacturing the construction materials, as in Figure 4.3. However, importing materials from overseas, such as specialty glulam from Europe or Chinese steel, does significantly increase the environmental cost. As seen in Figure 4.9, sourcing materials from China doubles the initial environmental cost, an increase of over $1500.

In a case study, Li and Froese (2016) found that a case-study building constructed using structurally-insulated panels (SIPs) did not have a smaller environmental impact than a standard building. This was because partially because the low environmental cost of hydroelectricity in Vancouver deflates the savings resulting from improved insulation, as shown in Section 4.6. Additionally, the SIPs used magnesium oxide sourced from China, which increased the emissions caused by transportation. The results above concerning hydroelectricity and material transportation costs support this conclusion.

Chapter 5: Conclusion

The work presented here is the next step in developing a program for holistic life-cycle assessment of buildings. This thesis describes the framework in which models for life-cycle costing may be implemented. BIM-compatibility and plug-and-play functionality features are also discussed.

Additionally, the basis for developing a probabilistic holistic life-cycle assessment tool is expounded upon, in comparison with existing design methodologies. An explanation on how to perform holistic life-cycle assessments in Rts is given, along with instruction on the selection of cost models and a discourse on discounting. Existing costing models are studied and described with background research and critiqued on the need for additional research. Additional models for construction cost estimation and preventative maintenance scheduling are also developed and implemented.

Finally, the results of a parametric study observing the effects of adjusting various parameters is described. The results support existing evidence that operating costs contribute a large portion of the total direct life-cycle cost. Additionally, the social cost of environmental impacts is high, supporting public policy that pushes for more environmentally-friendly construction. The sensitivities of the estimate of the building design life and discounting rate were studied to verify the functionality of the scenario model. Also, the depth of the cover concrete in the example building was varied to observe the effects on the total life-cycle cost, supporting current practice for concrete design. A study on different levels of energy use also supported the conclusion that energy-efficient buildings are also cost effective. Lastly, studies on material sourcing support recent literature in concluding that high transportation environmental costs reduce the environmental cost-effectiveness of using foreign materials for construction.

5.1 Future Work

Throughout the course of this research there was also discussion concerning how cost models should be organized. Cost models tend to be standalone, apart from the energy use models in conjunction with the environmental costing model. This facilitates plug-and-play functionality by allowing models to be easily replaced. However, some models necessarily violate this rule; for example, the transportation energy model requires input from another model for a labour-hour estimate. As with RGurvinderDirectConstructionCostModel from Section 3.4, not all construction cost models provide this. One solution might be that some cost models have additional requirements imposed on them; however, this further hampers the ease of developing new models to use in Rts. Another might be to require all cost models to be standalone; but this approach restricts models from providing useful information to each other. Whether or not establishing strict guidelines on cost modelling is even beneficial is unclear, as new models that do not meet the guidelines may be unfit for implementation.

As seen in Figure 3.2 and mentioned in Chapter 4, many costs are not yet modelled in Rts, such as user-experience costs. Gill (2017) described a preliminary model for estimating the cost of casualties, however this is not yet fully implemented in Rts. Additionally, this model uses fragility curves and does not take advantage of Rts' potential for detailed analysis. For example, the HAZUS technical manual (Federal Emergency Management Agency, 2015) provides information on the variation occupancy levels throughout a day. With detailed occupancy data, incorporation of finite element analysis results in a casualty-estimating model could allow for precise estimation of casualties in a building. Li, Zhai and Xie (2015) demonstrated the use of precise estimation of casualties involving explicit dynamic finite element analysis and occupant evacuation behaviour.

Additionally, the operating energy model does not calculate the daily energy use itself but takes it as an input. The current default value for daily energy use is based on the national average energy use intensity (Natural Resources Canada, 2017) and is only valid for the example building's size. Additional problems associated with this assumption were stated in Chapter 4. It is necessary to have a refined model for energy use to simulate the effects of improving building insulation, changing the building size, or adjusting the window placements. As mentioned in Section 3.9, eQuest's technical manual (James J. Hirsch & Associates, 2016) provides detailed models for estimating energy demand of a building.

Bibliography

Baumol, W. J. (1972). On taxation and the control of externalities. *The American Economic Review*, *62*(3), 307–322. https://doi.org/10.2307/1803378

Cement Association of Canada., & Canadian Standards Association. (n.d.). *Concrete design handbook.* Retrieved from http://webcat2.library.ubc.ca/vwebv/exportRecord.do

Cornell, C. A., & Krawinkler, H. (2000). Progress and challenges in seismic performance assessment.

Das, S., Chew, M. Y. L., & Poh, K. L. (2010). Multi-criteria decision analysis in building maintainability using analytical hierarchy process. *Construction Management and Economics*, *28*(10), 1043–1056. https://doi.org/10.1080/01446193.2010.501806

Ellingwood, B. R. (2008). Structural reliability and performance-based engineering. *Proceedings of the ICE - Structures and Buildings*, *161*(4), 199–207. https://doi.org/10.1680/stbu.2008.161.4.199

Enevoldsen, I., & Sørensen, J. D. (1994). Reliability-based optimization in structural engineering. *Structural Safety*, *15*(3), 169–196. https://doi.org/10.1016/0167-4730(94)90039-6

Faludi, J., Lepech, M. D., & Loisos, G. (2012). Using Life Cycle Assessment Methods To Guide Architectural Decision-Making for Sustainable Prefabricated Modular Buildings. *Journal of Green Building*, *7*(3), 151–170. https://doi.org/10.3992/jgb.7.3.151

Fearnside, P. M. (2016). Environmental and Social Impacts of Hydroelectric Dams in Brazilian Amazonia: Implications for the Aluminum Industry. *World Development*, *77*, 48–65. https://doi.org/10.1016/J.WORLDDEV.2015.08.015

Federal Emergency Management Agency. (2015). Hazus–MH 2.1: Technical Manual. *National Institute of Building Sciences and Federal Emergency Management Agency (NIBS and FEMA)*, 718. Retrieved from www.fema.gov/plan/prevent/hazus

Federal Reserve Bank of San Francisco. (2002). What is the difference between private and social costs, and how do they relate to pollution and production? Retrieved July 4, 2018, from https://www.frbsf.org/education/publications/doctor-econ/2002/november/private-social-costs-pollution-production/

Fowler, K. M., Rauch, E. M., Henderson, J. W., & Kora, A. R. (2010). *Re-Assessing Green Building Performance: A Post Occupancy Evaluation of 22 GSA Buildings*. https://doi.org/10.2172/1029438

Frangopol, D. M., & Maute, K. (2003). Life-cycle reliability-based optimization of civil and aerospace structures. *Computers and Structures*, *81*(7), 397–410. https://doi.org/10.1016/S0045-7949(03)00020-8

Gencturk, B., Hossain, K., & Lahourpour, S. (2016). Life cycle sustainability assessment of RC buildings in seismic regions. *Engineering Structures*, *110*, 347–362. https://doi.org/10.1016/j.engstruct.2015.11.037

Gill, G. (2017). *Probabilistic Cost Models for Holistic Design of Building Components*. MASc thesis, University of British Columbia, Vancouver, Canada.

Goh, B. H., & Sun, Y. (2016). The development of life-cycle costing for buildings. *Building Research & Information*, *44*(3), 319–333. https://doi.org/10.1080/09613218.2014.993566

Gordian. (2018). RSMeans Online. Retrieved from https://www.rsmeansonline.com/

Hammond, G. P., & Jones, C. I. (2008). *Inventory of Carbon and Energy Version 1.6a*. *ICE*.

Hopfe, C. J., Augenbroe, G. L. M., & Hensen, J. L. M. (2013). Multi-criteria decision making under uncertainty in building performance assessment. *Building and Environment*, *69*, 81–90. https://doi.org/10.1016/J.BUILDENV.2013.07.019

Huebner, G., Shipworth, D., Hamilton, I., Chalabi, Z., & Oreszczyn, T. (2016). Understanding electricity consumption: A comparative contribution of building factors, socio-demographics, appliances, behaviours and attitudes. *Applied Energy*, *177*, 692–702. https://doi.org/10.1016/J.APENERGY.2016.04.075

International Institute for Sustainable Development. (2017). *Costs of pollution in Canada: Measuring the impacts on families, businesses and governments*.

Islam, H., Jollands, M., & Setunge, S. (2015). Life cycle assessment and life cycle cost implication of residential buildings—A review. *Renewable and Sustainable Energy Reviews*, *42*, 129–140. https://doi.org/10.1016/J.RSER.2014.10.006

James J. Hirsch & Associates. (2016). eQuest. Retrieved from http://doe2.com/equest/

Kenley, C. R., & Armstead, D. C. (2004). Discounting models for long-term decision making. *Systems Engineering*, *7*(1), 13–24. https://doi.org/10.1002/sys.10051

Kim, J., Hong, T., Jeong, J., Koo, C., & Jeong, K. (2016). An optimization model for selecting the optimal green systems by considering the thermal comfort and energy consumption. *Applied Energy*, *169*, 682–695. https://doi.org/10.1016/J.APENERGY.2016.02.032

Kurnitski, J. (2013). *Cost Optimal and Nearly Zero- Energy Buildings (nZEB)*. (J. Kurnitski, Ed.). London: Springer London. https://doi.org/10.1007/978-1-4471-5610-9

Li, P. X., & Froese, T. M. (2016). Life-Cycle Assessment of High Performance, Low Cost Homes. *Icsdec 2016 - Integrating Data Science, Construction and Sustainability*, *145*, 1322–1329. https://doi.org/10.1016/j.proeng.2016.04.170

Li, S., Zhai, C., & Xie, L. (2015). Occupant evacuation and casualty estimation in a building under earthquake using cellular automata. *Physica A: Statistical Mechanics and Its Applications*, *424*, 152–167. https://doi.org/10.1016/J.PHYSA.2015.01.008

Mahoney, M., & Hanson, R. D. (2012). Seismic Performance Assessment of Buildings - Implementation Guide. *Fema P-58-2*, *2*(September), 357.

Mahsuli, M. (2012). *Probabilistic models, methods, and software for evaluating risk to civil infrastructure*. https://doi.org/10.14288/1.0050878

Mahsuli, M., & Haukaas, T. (2013a). Computer Program for Multimodel Reliability and Optimization Analysis. *Journal of Computing in Civil Engineering*, *27*(1), 87–98. https://doi.org/10.1061/(ASCE)CP.1943-5487.0000204

Mahsuli, M., & Haukaas, T. (2013b). Seismic risk analysis with reliability methods, part I: Models. *Structural Safety*, *42*, 54–62. https://doi.org/10.1016/j.strusafe.2013.01.003

Mahsuli, M., & Haukaas, T. (2013c). Seismic risk analysis with reliability methods, part II: Analysis. *Structural Safety*, *42*, 63–74. https://doi.org/10.1016/j.strusafe.2013.01.004

Marler, R. T., & Arora, J. S. (2004). Survey of multi-objective optimization methods for engineering. *Structural and Multidisciplinary Optimization*, *26*(6), 369–395. https://doi.org/10.1007/s00158-003-0368-6

McAllister, T. (2016). Research Needs for Developing a Risk-Informed Methodology for Community Resilience. *Journal of Structural Engineering*, *142*(8), C4015008. https://doi.org/10.1061/(ASCE)ST.1943-541X.0001379

McKenna, F. (2011). OpenSees: A Framework for Earthquake Engineering Simulation. *Computing in Science & Engineering*, *13*(4), 58–66. https://doi.org/10.1109/MCSE.2011.66

Means Engineering Staff. (2009). *RSMeans Estimating Handbook (3rd Edition)*. John Wiley & Sons.

Melchers, R. E. (2003). Probabilistic Model for Marine Corrosion of Steel for Structural

Reliability Assessment. *Journal of Structural Engineering*, *129*(11), 1484–1493. https://doi.org/10.1061/(ASCE)0733-9445(2003)129:11(1484)

Monteiro, I., Branco, F. A., Brito, J. de, & Neves, R. (2012). Statistical analysis of the carbonation coefficient in open air concrete structures. *Construction and Building Materials*, *29*, 263–269. https://doi.org/10.1016/J.CONBUILDMAT.2011.10.028

Natural Resources Canada. (n.d.). Residential Sector British Columbia1 Table 6: Space Heating Secondary Energy Use and GHG Emissions by Building Type | Natural Resources Canada. Retrieved April 10, 2018, from http://oee.nrcan.gc.ca/corporate/statistics/neud/dpa/showTable.cfm?type=CP&sector=res&juris=bc&rn=1&page=0

Natural Resources Canada. (2017). National Energy Use Database.

Noor, J. (2009). Hyperbolic discounting and the standard model: Eliciting discount functions. *Journal of Economic Theory*, *144*, 2077–2083. https://doi.org/10.1016/j.jet.2009.03.005

Nordhaus, W. D. (1994). *Managing the global commons : the economics of climate change*. MIT Press. Retrieved from http://webcat1.library.ubc.ca/vwebv/holdingsInfo?bibId=1004219

Nordhaus, W. D. (2007). A Review of the Stern Review on the Economics of Climate Change. *Journal of Economic Literature*, *XLV*(3), 686–702. Retrieved from https://search-proquest-com.ezproxy.library.ubc.ca/docview/213297644?pqorigsite=summon&accountid=14656

Nordhaus, W. D. (2011). *Estimates of the Social Cost of Carbon: Background and Results from the RICE-2011 Model*. Cambridge, MA. https://doi.org/10.3386/w17540

Revit. (2006). Building Information Modeling and Cost Estimating. *Autodesk*. Retrieved from http://images.autodesk.com/apac_grtrchina_main/files/aec_customer_story_en_v9.pdf

Robinson, L. A., & Hammitt, J. K. (2015). Research Synthesis and the Value per Statistical Life. *Risk Analysis*, *35*(6), 1086–1100. https://doi.org/10.1111/risa.12366

Royset, J. O., Der Kiureghian, A., & Polak, E. (2001). Reliability-based optimal structural design by the decoupling approach. *Reliability Engineering and System Safety*, *73*(3), 213–221. https://doi.org/10.1016/S0951-8320(01)00048-5

Sharma, A., Saxena, A., Sethi, M., Shree, V., & Varun. (2011). Life cycle assessment of buildings: A review. *Renewable and Sustainable Energy Reviews*, *15*(1), 871–875. https://doi.org/10.1016/j.rser.2010.09.008

Shindell, D. T. (2015). The Social Cost of Atmospheric Release. *Climatic Change*, *130*(2), 313–326. https://doi.org/10.1007/s10584-015-1343-0

Stern, N. (2007). *The Economics of Climate Change*. Cambridge: Cambridge University Press. https://doi.org/10.1017/CBO9780511817434

The ATHENA Institute. (2013). Athena impact estimator for buildings. Retrieved from http://calculatelca.com/software/impact-estimator/

The Qt Company. (2016). Qt Creator 4.0.2.

Tierney, K., & Bruneau, M. (2007). A Key to Disaster Loss Reduction. *TR News*, 14–18. https://doi.org/10.17226/23168

Tol, R. S. J. (2011). The Social Cost of Carbon. *Annual Review of Resource Economics*, *3*(1), 419–443. https://doi.org/10.1146/annurev-resource-083110-120028

Torres, H., Correa, E., Castaño, J. G., & Echeverría, F. (2017). Simplified Mathematical Model for Concrete Carbonation. *Journal of Materials in Civil Engineering*, *29*(10), 04017150. https://doi.org/10.1061/(ASCE)MT.1943-5533.0002001

Wen, Y.-K. (2001). Minimum lifecycle cost design under multiple hazards. *Reliability Engineering and System Safety*, *73*, 223–231. https://doi.org/10.1016/S0951-8320(01)00047-3

Yang, T., Moehle, J. P., & Stojadinovic, B. (2009). *Performance Evaluation of Innovative Steel Braced Frames*. *Simulation*.

Zhao, Y., & Jin, W. (2016). *Steel-Corrosion Induced Concrete Cracking*. Elsevier.

Zou, X. K., Chan, C. M., Li, G., & Wang, Q. (2007). Multiobjective Optimization for Performance-Based Design of Reinforced Concrete Frames. *Journal of Structural Engineering*, *133*(10), 1462–1474. https://doi.org/10.1061/(ASCE)0733-

9445(2007)133:10(1462)

Appendices

Appendix A Parametric Study Rts Input File

This input file has been formatted for viewing and is not suitable for use in Rts. Comments are included to explain the created objects.

```
// The mesh option is used by structural analyzers.

RConstant |ObjectName: officialMeshOption |CurrentValue: 3


// These time instances are used by the scenario model to indicate
the start and end times of the scenario.

RTime |ObjectName: startTime |Time: 2017-01-01 17:00:00.000

RTime |ObjectName: endTime   |Time: 2067-01-01 17:00:00.000


// LOCATIONS

// These location objects are used by the transportation model to
indicate the source of materials used for construction. steelSource2
and concreteSource2 represent sources in interior BC, while
steelSource3 and concreteSource3 represent an overseas source.

RLocation
|ObjectName: buildingLocation
|Latitude: 49.266514
|Longitude: -123.245556

RLocation
|ObjectName: concreteSource1
|Latitude: 49.271192
|Longitude: -123.133112

RLocation
```

```
|ObjectName: steelSource1
|Latitude: 49.316532
|Longitude: -123.091248

//RLocation
|ObjectName: concreteSource2
|Latitude: 49.220098
|Longitude: -122.557000

//RLocation
|ObjectName: steelSource2
|Latitude: 49.220098
|Longitude: -122.557000

//RLocation
|ObjectName: concreteSource3
|Latitude: 39.809403
|Longitude: 116.446058

//RLocation
|ObjectName: steelSource3
|Latitude: 39.809403
|Longitude: 116.446058



// BUILDING

// The BIM object includes information required by statistics-based
models, such as the construction type. Notice its use in most of the
later cost models.

RBIM
|ObjectName: theBIM
|Location: buildingLocation
|IfcFile: stevesSaloon.ifc
|TimeOfConstruction: startTime
|TimeOfDemolition: endTime
|LoadBearingSystem: MomentFrame
|ConstructionMaterial: ReinforcedConcrete
|NumberOfStoreys: 3
|FootprintArea: 691
|OccupancyType: Services
|PlanIrregularity: true
```

```
|VerticalIrregularity: false
|SoftStorey: false
|Opening: false
|ShortColumn: false
|Pounding: false
|Retrofitted: false



// COST MODELS

// The construction cost model here is described in Section 3.6 and
returns a labour response for some energy use models. Material
volumes are also passed to the material cost model for separate
costing.

RSeadonDirectConstructionCostModel
|ObjectName: theConstructionCostModel
|BIM: theBIM

REnergyUseInManufacturingModel
|ObjectName: theManufacturingEnergyModel
|BIM: theBIM

// The locations in this model were varied in the parametric study
to study the effects of the construction material source.
Additionally, it uses the labour response produced by the
construction cost model. Note that the study building did not have
timber components; the source given here is not used.

REnergyUseInTransportationModel
|ObjectName: theTransportationEnergyModel
|BIM: theBIM
|TotalWorkerHours: theConstructionCostModelLabourResponse
|HoursPerShift: theHours
|ConcreteSource: concreteSource1
|SteelSource: steelSource1
|TimberSource: steelSource1

REnergyUseInOperationModel
|ObjectName: theOperationEnergyModel
|BIM: theBIM

REnergyUseInConstructionModel
```

```
|ObjectName: theConstructionEnergyModel
|BIM: theBIM
|TotalWorkerHours: theConstructionCostModelLabourResponse

RGurvinderDemolitionCostModel
|ObjectName: theDemolitionCostModel
|BIM: theBIM

RSeadonPreventativeMaintenanceModel
|ObjectName: theMaintenanceModel
|BIM: theBIM

// Again, note how this model takes responses from both the
maintenance and construction cost models. This model represents all
actions involving the purchase of materials and may be used in the
future for building damage repair models.

RDirectCostOfMaterialsModel
|ObjectName: theMaterialCostModel
|BIM: theBIM

// Each of the fuel-type lists here takes the corresponding
responses from the energy models. Not all energy models produce
energy responses for every fuel type.

RShindellEnvironmentalCostOfEnergyModel
|ObjectName: theShindellCostModel
|BIM: theBIM
|JouleCoalList: theManufacturingEnergyModelJouleCoalResponse;
theTransportationEnergyModelJouleCoalResponse;
theDemolitionCostModelJouleCoalResponse
|JouleDieselList: theManufacturingEnergyModelJouleDieselResponse;
theTransportationEnergyModelJouleDieselResponse;
theDemolitionCostModelJouleDieselResponse;
theConstructionEnergyModelJouleDieselResponse
|JouleElectricityList:
theManufacturingEnergyModelJouleElectricityResponse;
theTransportationEnergyModelJouleElectricityResponse;
theDemolitionCostModelJouleElectricityResponse;
theOperationEnergyModelJouleElectricityResponse
|JouleFuelOilList: theManufacturingEnergyModelJouleFuelOilResponse;
theTransportationEnergyModelJouleFuelOilResponse;
theDemolitionCostModelJouleFuelOilResponse
```

```
|JouleGasolineList:
theManufacturingEnergyModelJouleGasolineResponse;
theTransportationEnergyModelJouleGasolineResponse
|JouleLPGList: theManufacturingEnergyModelJouleLPGResponse;
theTransportationEnergyModelJouleLPGResponse
|JouleNaturalGasList:
theManufacturingEnergyModelJouleNaturalGasResponse;
theTransportationEnergyModelJouleNaturalGasResponse;
theOperationEnergyModelJouleNaturalGasResponse;
theDemolitionCostModelJouleNaturalGasResponse

// The constant here represents the length of a workday, used by the
transportation energy model to calculate the number of trips for
workers.

RConstant  |ObjectName: theHours |CurrentValue: 8.0



// ORCHESTRATING ANALYSIS MODELS

// The MaxTimeGap attribute indicates how often the models should be
checked for updating costs, in addition to pre-set trigger times
such as the start time.

RScenarioModel
|ObjectName: scenarioModel
|InputParameterList: theConstructionCostModelResponse;
theDemolitionCostModelResponse; theShindellCostModelResponse;
theOperationEnergyModelResponse; theMaintenanceModelResponse;
theMaterialCostModelResponse
|StartTime: startTime
|EndTime: endTime
|MaxTimeGap: 365
|RealInterestRate: 0.05
|OutputLevel: Medium

// The sampling model accumulates and charts the results of the
scenario model analyses

RSamplingModel
|ObjectName: theSamplingModel
|OutputLevel: Medium
|InputParameter: scenarioModelResponse
```

```
|Threshold: 0.0
|ProbabilityTransformation: theProbTransformation
|TargetCov: 0.00002
|MaxSamples: 100
|PlotInterval: 10
|RandomNumberGenerator: theGenerator


// METHODS

RIndependenceProbabilityTransformation
|ObjectName: theProbTransformation
|ProbabilityDistributions: theProbDist

RInHouseRandomNumberGenerator          |ObjectName: theGenerator

RInHouseProbabilityDistributions       |ObjectName: theProbDist
```